Vysoké učení technické v Brně
Fakulta strojního inženýrství
Ústav konstruování

Brno University of Technology
Faculty of Mechanical Engineering
Institute of Machine and Industrial Design

BIOCHEMICAL PROCESS OF LUBRICANT FILM FORMATION IN JOINT REPLACEMENT

RISHA RUFAQUA, MSc, MBA.

Pojednání ke státní doktorské zkoušce
Discourse on the dissertation thesis

Brno 2020

Vysoké učení technické v Brně
Fakulta strojního inženýrství
Ústav konstruování

Brno University of Technology
Faculty of Mechanical Engineering
Institute of Machine and Industrial Design

BIOCHEMICAL PROCESS OF LUBRICANT FILM FORMATION IN JOINT REPLACEMENT

Risha Rufaqua, MSc, MBA.
Autor práce
Author

doc. Ing. Martin Vrbka, Ph.D.
Vedoucí práce
Supervisor

Pojednání ke státní doktorské zkoušce
Discourse on the dissertation thesis

Brno 2020

CONTENTS

1 ABSTRACT

To clarify the biochemical reactions of the formation of the lubricating film between head and the cup of the joint replacement is the main objective of this project. The chemical composition of synovial fluid along with frictional coefficients will be predominantly considered to explain the development of film on the ball and the experiments will be conducted in ball-on-cup configuration. Where the balls are made from respectively cobalt chromium molybdenum alloy and ceramics. The cups are of respectively optical glass, ceramic and polyethylen. Synovial fluid constituents such as: albumin, γ-globulin, hyaluronic acid and some model synovial fluids in the experimental set up will be considered as the reactant of this process. To analyze the product of the reaction, Raman spectroscopic method will be used to measure non-polar bonds among the protein of synovial liquid. The expected results could have significant information for the development lubricating film within the joint replacement.

2 RESEARCH BACKGROUND

The synovial fluid (SF) has a complex biochemical composition. Proteins derived from the blood plasma and cells within the joint tissues (such as synovium, cartilage, ligament, and meniscus) are contained in SF of an articulating joint [1]. This highly efficient water-based tribological system is optimized to provide low friction and wear protection at both low pressures as well as high pressures or loads and also sliding velocities for the entire life of a human [2]. As for mobility in the skeletal system, synovial joints act as bearings and SF is responsible for the lubrication of these bearings through various mechanisms [3]. The molecules participating in joint lubrication are engaged mainly in providing an effective surface lubricant reducing the friction and excluding wear damage to the rubbing or shearing surfaces [2].

Containing proteins, phospholipids (PLs), hyaluronic acid (HA), cholesterol and glycoproteins, the SF composes a complex mixture of large and surface-active molecules [4, 5]. However, the proteome composition of healthy SF and its different components' cellular origins are yet to be understood completely [1].

Among functions of SF lies biological lubrication within the joint and it also acts as a biochemical pool for nutrients and regulatory cytokines outpour. On the other hand, tribological performance of cartilage cannot be featured only with a single mechanism. Rather, multiple functions of lubrication take place mutually. Normal loads, shear stresses, and rates change are provided by articulating cartilage surfaces when lubrication is optimum, yielding low-friction and low-wear properties. At the beginning of bio-tribology research, Dowson and Walker et.al. [6], had provided the idea that the cartilage surfaces are prevented from contacting each other primarily because of the formation of trapped pools of lubricant. An acid-protein complex is formed as a protective gel due to fluid compressed and concentrated between cartilage surfaces. Walker, Dowson et.al. [6], termed this combination of trapped pool and fluid concentration as "boosted lubrication". Proteoglycan 4 (PRG4), HA, and surface active phospholipids (SAPL) contribute to the total arrangement of the system. The proteins are produced from synovium, cartilage, ligament and meniscus, while the structure of the proteins and their functions are attributed to Pls directly. On the other hand, HA contributes more as a potential boundary lubricant for cartilage and shows a small amount of lubrication activity. [2, 6-8].

In a model described by Blewis et al. [7], SF is compared to an ultra-filtrate of plasma, which has the ability of filtration through the synovial membrane with chondrocytes in articular cartilage and synoviocytes in synovium secrete lubricants.

Within the synovial space, SF is accumulated and separated by the semi-permeable synovial lining. The chemical regulation is assumed to be controlled by lubricant concentration, as secreted by chondrocytes and synoviocytes [7].

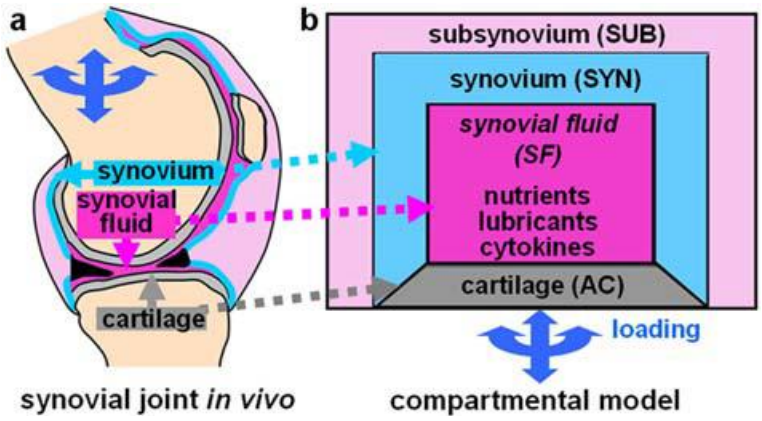

Fig. 1 (a) Synovial joints composed of cartilage, synovium, and synovial fluid; (b) communicating compartments are present in synovial fluid, while lubricant secretion is regulated by chemical and mechanical factors [7]

Therefore, SF also plays a transporting role of the boundary lubricant to its site of adsorption. Being one of the essential elements of SF, HA produces a cross-linked network by complex with glycoprotein lubricin, whose solutions are slippery to the touch. This network complex provides wear prevention mechanism of joints and is also responsible for boundary lubrication (chemically) [2, 9].

Another element abundant in SF is the SAPL (surface-active phospholipids). These small molecules function as binders of amino acid groups. Protein chains are constructed by amino acid groups in proteoglycans such as lubricin. Lubricin is formed by a long, heavily glycosylated, mucinous domain, separating two somatomedin domains at the N-terminus and a haemopexin region at the C-terminus. The total amount of lubricin in SF is small, but it helps to avail boundary lubrication as well as lubrication properties, transporting and anchoring of PLs to the cartilage surface and the friction coefficient of different area of articular cartilage in a substantial amount. It also contributes essentially to chondroprotective properties of articular cartilage; by interaction with HA via dissipation of shear-induced energy, this activity is further increased. Thus, effective biolubrication is provided by lubricin in the presence of other major components in SF [9, 10].

The principal element of SF is PLs, amounting in the normal joint constitution to about 61%. Being the main phospholipid component, phosphatidylcholine is extremely surface-active due to large saturation of joint PLs [9].

Albumin, the most abundant protein of SF, shows affinity to hydrophobic surfaces such as OH-terminated surfaces. Adherence of albumin to artificial surfaces may thus be regulated by altering the pH value. Therefore, for lubrication of articular surfaces and interaction with other components albumin plays an important role. On the other hand, globulin activity is more focused on boundary lubrication. At low speeds globulin plays a role of pH-independent boundary lubricant. When speed is higher, boundary lubrication by globulin depends on pH, which in turn helps in producing hydrodynamic or mixed lubrication [10].

Thus the chemical behaviour and friction and wear properties of the joints are controlled by prime constituents of human SF, which are proteins such as serum albumin and γ-globulin, PLs, and HA [11, 12].

Erosion of articulating cartilage surfaces may occur due to arthritis if there is a lack of proper SF lubricating system or any disruption of chemical environment within synovial joint takes place. In damaged joint SF normal electrostatic interactions are not workable, probably due to chemical-changes-induced secondary structure modification of the proteins [7, 13].

Differences in SF composition were observed for normal knee joint, patients without replacement of joint, patients with primary arthroplasties and patients with revisions of total hip and knee arthroplasties [11]. The proteins naturally occurring in SF can vary in concentration. In particular, HA, protein and phospholipid concentrations varied widely in patients undergoing the joint replacement [9, 14]. The thickness of lubricant film within hip prostheses is hypothesized to influence particular proteins [15].

It has also been stated that concentrations of bovine serum albumin and γ-globulin manipulate the frictional behaviour of the CoCr femoral head [16]. The optimum tribological performance of joint replacement would also be subject to combination of composition, microstructural condition and manufacturing process of the alloy [17].

In general, friction is approximately two times higher for metal pair compared to the ceramic [18]**,** and thicker film is adsorbed by alumina ceramic compared to zirconia toughened alumina ceramic or metal [19].

To explain biochemical reactions underlying the lubricating film formation, Raman spectroscopy can be used to study the chemical bonding among the protein constituents. Vibrational fingerprint provided by Raman spectroscopy can be used to analyse or identify the components present [20]. In addition, correlation between the level of PLs and proteins exists and can be deduced from Raman spectra [8]. The technique has also been previously used to distinguish between healthy SF and SF changes in osteoarthritis (OA) patients as well as to OA subchondral bone matrix change detection [13, 20]. By Raman spectroscopy it is also found that for zirconia toughened alumina ceramic wear was the main cause of the in vivo tetragonal-to-monoclinic zirconia transformation [21].

This contribution aims to clarify the chemical reaction of SF components due to the film formation of the joint replacement along with the film mechanical properties.

3 STATE OF THE ART REVIEW

3.1 Film formation and thickness of the film of lubricants

The publications related to Film thickness are also includes either pH dependency or Kinematic conditions of synovial fluid protein content as lubricants. Representative papers are introduced as follows.

[15] **Nečas David, Martin Vrbka, Filip Urban, Ivan Křupka & Martin Hartl.** "The effect of lubricant constituents on lubrication mechanisms in hip joint replacements," *Journal of the Mechanical Behavior of Biomedical Materials*, 55, 2016, 295-307.

The research was focused on thickness of lubricant film for specific proteins on hip joint replacements and interfacial lubrication process. Different kinematic conditions such as, under pure rolling, partial negative and partial positive sliding on film formation were considered in this experiment during measurement of film thickness.

Materials and Methods

To observe lubricant film thickness a conventional ball-on-disc tribometer was used including a contact pair of cobalt chromium molybdenum **(**CoCrMo) femoral head of nominal diameter of 28mm and the glass disc (BK7) coated with a thin chromium layer.

Test lubricant were protein solution in phosphate- buffered saline (PBS) included bovine serum albumin (BSA) (Sigma-Aldrich A7030) doped by Rhodamine-B isothiocyanate (Sigma- Aldrich 283924) and γ-globulin from bovine blood (Sigma Aldrich-G5009) stained by Fluorescein-5-isothiocyanate (Sigma-Aldrich F7250). The final protein concentration was 198.5 mg/ml. The ratio of albumin (A) and γ-globulin (G) was used as A:G 2:1, the total concentration of A and G in model fluid was 7mg/ml and 3.5mg/ml. An optical imaging system consists of mercury lamp for illumination, microscope, digital camera, and PC set up was used to observe the contact.

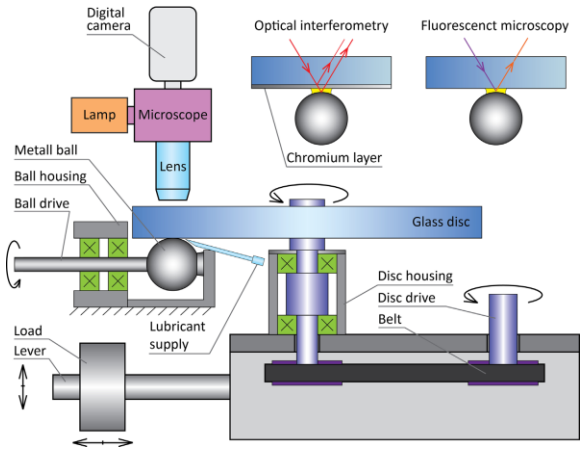

Fig. 2 Scheme of ball on disk experimental approach [15]

To measure film thickness two types of technique were used:

a. Thin film colorimetric interferometry and
b. Fluorescent microscopy in combination with the optical method

During the measurement of film thickness the contact surface of glass disc was considered as optically smooth.

Results

The protein film formation was observed as a complex and time/distance depended process. The film gradually increased under pure rolling conditions while there was no substantial scatter in results.Under partial negative sliding, where the ball was faster than the disc,the thickness of film was generally very thin. Whereas under positive sliding conditions the most scattered results were obtained when the disc was faster than the ball. The increase in mean speed usually obtained to the increase of thickness of film. But under positive sliding the effect of speed was opposite. Thus the maximum value for 5.7 mm/s was more than 120 nm, whereas under higher speed, it was only around 40 nm.

The increase of lubricant film can be imputed specifically to the increase of albumin. A very thin layer of γ-globulin is assumed adsorbed primarily on to rubbing surfaces, enabling the albumin to adsorb on it and to create a layer structure.

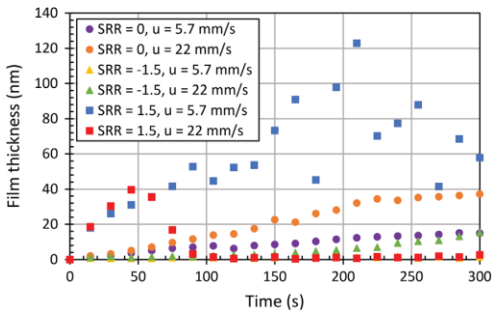

Fig. 3 Comparison of film thickness measurements by thin filmcolorimetric interferometry for various operating conditions [15]

Conclusions

In this study the lubricant film formation was attributed in meaning of particular proteins. It is comprehended that, the thickness of film is formed predominantly due to the presence of albumin, specifically under pure rolling and positive sliding conditions. Hence under negative sliding, the film thickness is strongly dependent on time and sliding distance. At higher speeds the film is mainly caused by γ-globulin. γ -globulin forms a very thin protein layer on the base material, while the albumin adsorbs onto the layer and therefore, increases the total film thickness. Thus in most cases, albumin contributes to increasing the total film thickness.

[22] **Parkes Maria, Connor Myant, Philippa M. Cann & Janet S.S. Wong,** "Synovial Fluid Lubrication: The Effect of Protein Interactions on Adsorbed and Lubricating Films," *Biotribology*, 1–2, 2015, 51–60.

Film formation impact of protein content of model synovial fluids under static and rolling condition and correlation with changing properties were studied in this research. Two different pH and six different compositions of synovial fluids were used to observe the filmthickness.

Materials and Methods

Adsorption of BSA and bovine gamma globulin (BGG) on silica and chromium surface was observed at pH 7.4 and 8.1. To keep the buffer chemistry unchanged Tris Saline buffer was used to prepare all solutions. The pH were adjusted to either pH 7.4 or 8.1 using sodium hydroxide (NaOH) or hydrogen chloride (HCl), to mimic the pH values represent a healthy synovial fluid pH and the increased pH of osteoarthritic and periprosthetic SF. Without further purification BSA (Sigma Aldrich, A7906, ≥98% agarose gel electrophoresis, lyophilized powder) and BGG (Sigma Aldrich, G5009, ≥99% agarose gel electrophoresis) were used. The concentrations 10 mg ml^{-1} and 2.4 mg ml^{-1} of BSA and BGG respectively were used at which are within the physiological range for these proteins in healthy SF.

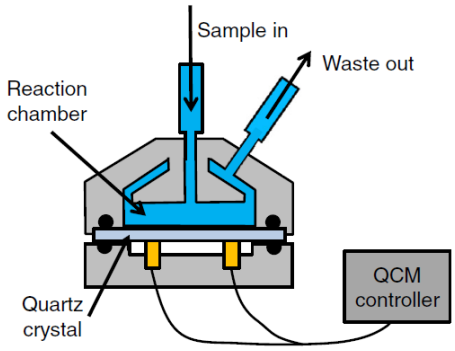

Fig. 4 Schematic of Quartz Crystal Microbalance with flow cell [22]

A ball on flat device were used for adsorption measurement in static condition. Under pure rolling condition, optical interferometry was used to observe the effect of protein content on lubricant film thickness on silica/CoCrMo interface. The dynamics of protein adsorption and the nature of the adsorbed film were analysed by Quartz Crystal Microbalance, which uses a quartz crystal that is electrically stimulated to oscillate at its resonant frequency.

Results

Under static condition more BGG was assumed to be adsorbed in all cases, when the concentration of BGG and BSA in single protein solutions was 2.4 mg/ml and 10 mg/ml respectively. Thus eventually BGG adsorption occurs at a higher rate than BSA adsorption.

A thicker film is formed in the case of chromium surface or detrimental as for silica surface with increasing pH. For final adsorbed mass the pH change is more effective for BGG films on silica and less effective on chromium surfaces. An increase of pH from 7.4 to 8.1 adsorbed mass reduced 10% and 39% for BSA and BGG proteins

respectively on silica. But in chromium surface, an increase of pH increases in adsorbed mass for both BSA (15%) and BGG (9%) films.

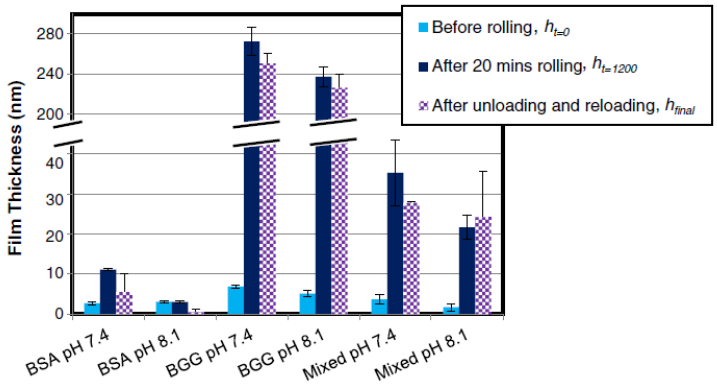

Fig. 5 Average measured film thickness for all protein solutions at pH 7.4 and 8.1 [22].

After analysis of both static results from QCM test and rolling adsorption results show that the average film thickness in protein solutions BGG is thickest and BSA is thinnest and while using the mixtures the result found some where in between BGG and BSA.

Conclusions

Therefore it could be concluded that protein layers are thicker under rolling than statical condition. Film formation depends on Protein content and the pH of solution in both conditions. BGG and mixed protein bounds more strongly than BSA. Bovine gamma globulin forms much thicker deposited layers compare to BSA.

[4] **Fan Jingyun, Connor Myant, Richard Underwood & Philippa Cann.** "Synovial fluid lubrication of artificial joints: protein film formation and composition," *Faraday Discussions*,156, 2012, 69-85.

In this paper film thickness and wear measurements for various model SF solutions of different pH according to diseased or post operative SF solutions. Film formation mechanisms were determined in imitation of an adsorbed surface film and a high viscosity gel.

Materials and Methods

Thin film optical interferometric test device was used to analyse film thickness and wear tests. The experiment conducted within glass disc of surface roughness 15nm and CoCrMo surface of surface roughness 20nm. The measurement of film thickness took place either at constant speed as a function of time or sliding distance or for changing speed. A range of model synovial fluids of variety of pH of 7.4 to 8.5 and variety of protein content of (10mgml^{-1} to 30 mgml^{-1} albumin) were utilized.

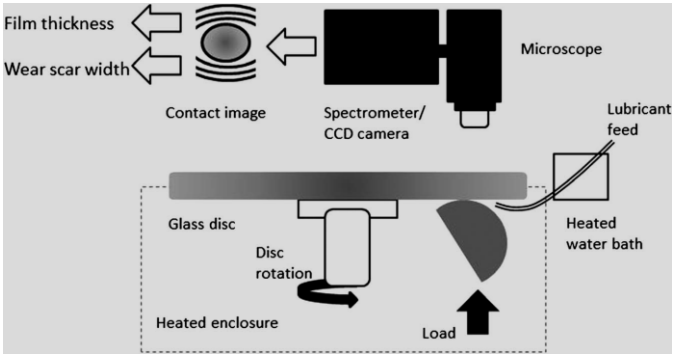

Fig. 6 Schematic diagram of film thickness and wear measurement [4]

25% bovine serum fluids were measured high shear rate viscosity of in the range 0.002–0.003 Pa s. The femoral head surface was examined before and after testing using an optical microscope and optical interferometric surface profilometer.

Results

Over 720s film thickness gradually increases with time, at 10 mms^{-1} it was approximately 35 nm which was apparently increased from 0 mms^{-1} approximately 10 nm. In all tests the thickest films were formed by globulin containing fluids. A discrete yellow regions of a boundary film was formed initially within the Hertzian contact. With progression these spots attached and changed into dark brown/red indicating a local increase in film thickness. For the low-protein solutions film thickness increased with sliding speed whereas the high protein solutions showed the opposite effect.

The relationship of pH and film thickness veried against with over 20 min are as follows:

0 mm s^{-1} pH 8.0, pH 8.5 >> pH 7.4
20 mm s^{-1} pH 7.4 > pH 8.0 > pH 8.5

Wear scar diameter for the different solutions were also changed, the wear ranking was as follows:

pH 7.4 < pH 8.0 ~ BCS 25 < pH 8.5
Least Highest

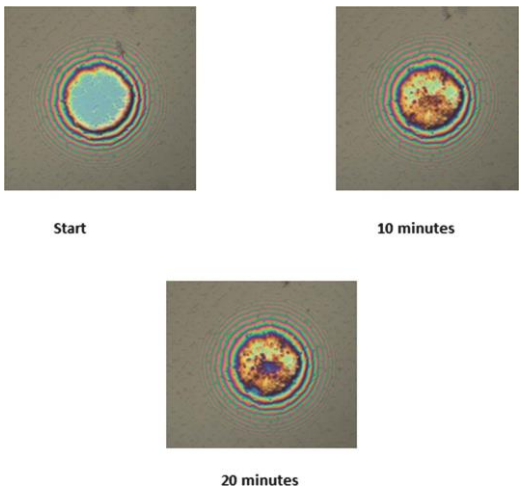

Fig. 7 SLIM images from a static, loaded contact with an albumin/globulin fluid present. The initial blue colour is due to the silica spacer layer. The formation of a separating film is seen initially as yellow regions and then brown/red areas [4]

Conclusions

Film formation signifies by two distinct mechanisms: boundary lubrication mechanism and high viscosity gel mechanism. The agglomerated protein forms organic deposits on the surface of implants. Wear mechanism is designated through tribocorrosion process, with higher pH, wear increases. The chemistry within synovial fluid has a significant effect on wear and failure of joint replacements.

[17] **Vrbka Martin, Ivan Křupka, Martin Hartl, Tomáš Návrat, Jiří Gallo & Adéla Galandáková**, "In situ measurements of thin films in bovine serum lubricated contacts using optical interferometry, " *Proceedings of the Institution of Mechanical Engineers, Part H: Journal of Engineering in Medicine*, 228(2), 2014, 149-158.

Ball on disc and lens on disk configuration were used for metal and ceramic ball with silica and chromium layer on glass disk, for bovine serum (BS) lubricant considering as a function of artificial hip joint. Film thickness was measured by optical interferometry as a function of time. The BS film formation was observed and film thickness was measured through various test configurations.

Materials and Methods

BS (Sigma–Aldrich B9433, protein concentration 55.5 mg/mL) of 25% with a total protein content of 13.9 mg/mL was prepared. A thin semi-reflective chromium layer with a different thickness was used to coat the lower surface of the glass disc or lens and the upper side had an antireflective coating. For some experiments, A silica layer (SiO2) with additional thickness of 150 nm was also used for some experiments on the chromium layer of glass disc. 36 mm and 28mm diameter CoCrMo balls and 32mm diameter Al_2O_3 balls were utilized for the experiment.

Surface topography of the metal and ceramic balls were observed using the optical measurement method based on phase shifting interferometry by using apparatus Bruker Contour GT-X8. Film thickness was studied as a function of time for various material combinations of contact surfaces by using optical test rig in which a circular contact is realized between a glass disc or lens and a metal or ceramic head of total

hip joint replacement. A high-speed complementary metal-oxide semiconductor (CMOS) digital camera was used to obtained chromatic interferograms and evaluated using a thin film colorimetric interferometry.

Results

Formation and evolution of film thickness in the whole contact zone dependent on time. Film thickness measurements for three values of slide-to-roll ratio (Σ = 0, 1.5 and -1.5) are displayed for CoCrMo ball having diameter of 28 mm and for mean speed of 5.7 mm/s. Average film thickness from the central area of the contact zone, and the marked grey region (0–180 s) represents the time of BS supply to the contact zone (Fig. 8). The film thickness increases gradually with time under pure rolling conditions (Σ = 0), and at the end of measurement central film thickness was 25nm. While the disc is faster than the ball, under rolling/sliding conditions, (Σ = 1.5), at first, the film thickness increases rapidly, and then the effect is lost when the maximum film thickness about 140 nm is reached and the film thickness starts to decrease, and finally the film thickness drops to a few nanometres.

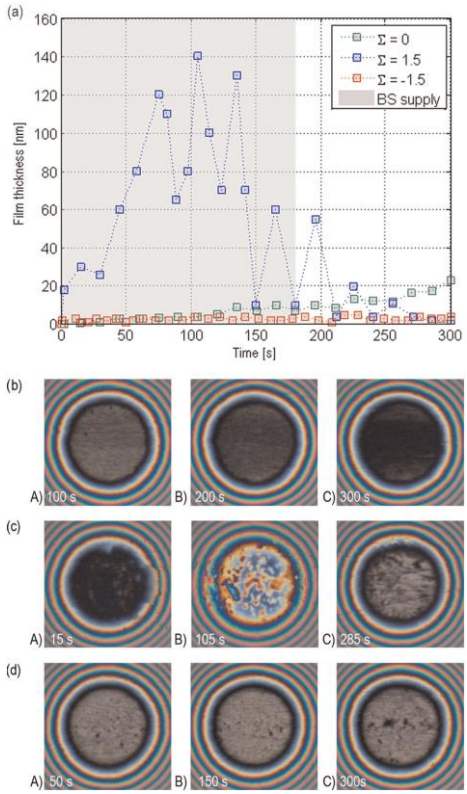

Fig. 8 Film thickness behaviour as a function of time for three values of slide-to-roll ratio (Σ) and mean speed of 5.7 mm/s (a) Central film thickness development. Chromatic interferograms: (b) Σ = 0, (c) Σ = 1.5 and (d) Σ = 21.5 [23]

Protein film formation can also be connected with the disc geometry and its movements and can influence the obtained results within the optical test rig. Another experiment was performed where both the disc with chromium layer and the CoCrMo ball were fully bathed in BS lubricant. During slow rotation of the disk BS on its surface can change properties – it can be dried out before entering the contact again.

Measurement of wettability of ball and disc contact surfaces was found as below chart:

Table. 1 Measurement of wettability of ball and disc contact surfaces [23]

Contact surface	Contact angle (°)
Ball, CoCrMo	71.6 ± 2.5
Ball, Al_2O_3	60.4 ± 1.7
Glass disc, Cr layer	94.5 ± 2.5
Glass disc, SiO_2 layer	28.7 ± 2.0
Glass disc, SiO_2 layer + hydrophobic modification	100.5 ± 2.4

Conclusions

The present results suggest that glass disc covered by a chromium layer showing hydrophobic behaviour formed thicker lubricating film. On the other hand, silica layer in same condition showed hydrophilic behaviour. Due to hydrodynamic effect, a thin film was formed on the silica layer. Wettability has no effect on protein film formation, while kinematic condition and conformity of the contact surface has fundamental effect. Due to protein aggregation film formed within the ball on disc configuration. On the contrary ball on lens configuration hydrodynamic effect leads to film formation.

[24] **Parkes Maria, Connor Myant, Philippa M. Cann & Janet S.S. Wong,** "The effect of buffer solution choice on protein adsorption and lubrication," *Tribology International,* 72, 2014, 108–117.

The dependence of the protein adsorption kinetics and film formation on buffer selection and pH impact explains by this study. The experiment pursued both under static and rolling conditions respectively with different pH.

Materials and Methods

Eight buffer solutions were prepared of pH 5.6, pH 7.4 that represents healthy synovial fluid and 8.1 representing osteoarthritic diseased fluid. As protein, BSA, (Sigma Aldrich, A7906, Z98% agarose gel electrophoresis, lyophilized powder) was utilized and all solutions are prepared with a concentration of 10 mg ml^{-1}. To observe the adsorption properties of BSA of Quartz Crystal Microbalance was used. Under static condition adsorption of proteins were investigated on silica coated quartz crystal. Under rolling condition, ball-on-flat device was used and film thickness or protein solution was measured by thin film optical interferometry.

Results

Under static condition there were initial rapid change in both frequency and resistance for all protein solutions enter the flowcell. For pH 5.6 the adsorbed layers were relatively rigid initially. Further adsorption of proteins induced viscous behaviour of the film, perhaps it took place with hydrated salts and water. The films were viscoelastic through out their formation for pH 7.4. Tris saline pH 8.1 results in adsorbed films that are highly viscous initially, but reduces in viscous nature as adsorption progresses. Therefore the final amount of adsorbed protein is similar in all buffers, the rate of protein adsorption is different.

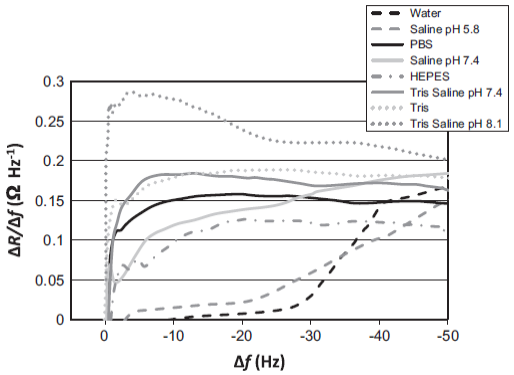

Fig. 9 Changes in the ratio ΔR/Δf plotted against changes in frequency for all protein solutions giving an indication of the elastic properties of the adsorbed protein film [24]

Under rolling condition film thickness were measured are17nm , 9nm, 11nm and 3nm respectively for saline pH 5.8, saline pH7.4, Tris saline pH 7.4 and TRIS saline pH8.1 protein solutions.

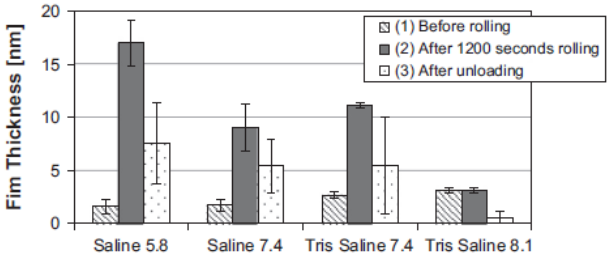

Fig. 10 Average film thickness (1) after static adsorption and before rolling, (2)after 1200 s rolling and (3)after unloading and reloading [24]

Conclusions

The aspect of buffer depends on pH within static condition. Both in static and rolling conditions pH has an impact on film formation. At lower pH, protein adsorption observer initially rigid and relaxed, with time rate increased. At pH 7.4 or lower, thicker protein film formed in rolling condition. The film found non-uniform and irregular deposition of protein. At higher pH initially, viscoelasticity is higher, also uniform and consistent film formed at static condition.

[19] **Nečas David, M. Vrbka, D. Rebenda, J. Gallo, A. Galandáková, L. Wolfová, I. Křupka & M. Hartl,** "In situ observation of lubricant film formation in

THR considering real conformity: The effect of model synovial fluid composition, ” *Tribology International*, 117, 2018, 206-216.

By using variuos composition of synovial fluids within pendulum hip joint simulator lubricant film formation on metal and ceramic femoral heads were analyzed.

Materials and Methods

In the experiment the contact of the CoCrMo metal head and BIOLOX®delta and BIOLOX®forte ceramic heads sliding were used against glass acetabular cups (BK7) approaching the contact conditions in hard-on-hard hip implants. Within pendulum hip joint simulator the utilized lubricants were 25% BS, two types of model SF (SF1 and SF2) mimic the same of pateints of total joint replacements (TJR) and without TJR respectively, albumin, γ- globulin and HA with two different concentration. While the film thickness was evaluated as a fuction of time using optical interferometry by the method of thin film colorimetric interferometry. Initially, static tests, aimed on the effect of material and load on adsorption, were conducted. For metal femoral head dynamic swinging tests were also conducted.

Results

During static adsorption test with metal head total film thickness of BS was observed at final stage more than doubled compared to model SF2 and the film for model SF1 filmthickness was found approximately placed in the middle.

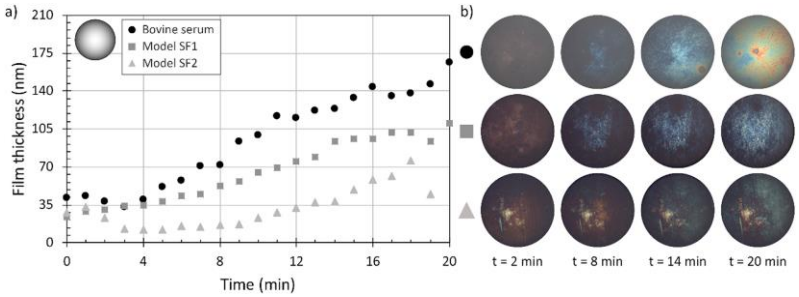

Fig. 11 a) Static test - film thickness of adsorbed film as a function of time for 36 mm metal head and various model fluids. b) Chromatic interferograms taken during the experiment; from the top: BS, model SF1, model SF2 [19]

In case of using BIOLOX®forte both model fluids were observed relatively similar behaviour with a slight increasing tendency of the adsorbed layer, On the other hand, BS formed thicker layer the maximum thickness reached almost 210 nm.

BIOLOX®delta were analysed under five different levels of load, where the thinnest film was detected for the highest load and the thickness was half compared to the lowest load.

Conclusions

From the analysis practically it is proved that the film formation is affected by composition of model fluid. Adsorbed film thickness enhances independently of the head material. Higher concentration of HA and PLs causes the decreasing of the film thickness.

3.2

3.2 Synovial Joint Relationship with Mechanical Properties

In below researches frictional coefficient of hip joint replacement were studied mostly along with boundary lubrication and also with protein adsorption on surface.

[16] **Duong Cong-Truyen, Jae-Hoon Lee, Younho Cho, Ju-Suk Nam, Hyong-Nyun Kim, Sang-Soo Lee & Seonghun Park,** "Effect of protein concentrations of bovine serum albumin and γ-globulin on the frictional response of a cobalt-chromium femoral head," *Journal of Materials Science: Materials in Medicine.* 23(5), 2012, 1323-1330.

This study was focused on concentration levels dependency of BSA and γ-globulin influence on the lubricating ability as well as the frictional coefficients of CoCrMo hip prostheses.

Materials and Methods

Sections of the retrieved CoCrMo femoral head from revision surgery due to aseptic loosening 10 years after hip arthroplasty was lubricated with several concentrations of BSA and γ-globulin. By using a small amount of cyanoacrylate glue the sample was glued on top of a cylindrical flat plate (1 mm thickness and 19 mm diameter). prepared solutions were three different types at different concentrations. First, As a control solution PBS (Ref. P5493, Sigma-Aldrich) was and then BSA (Ref. A2153, Sigma-Aldrich) was utilized as a lubricant at concentrations of 10, 20, 30, and 40 mg/ml in PBS. And finally, BGG (Ref. 5009, Sigma-Aldrich) at concentrations of 2.5, 5.0, 7.5, and 12.5 mg/ml in PBS solution was availed.

Atomic force microscopy (AFM) (XE 70, Park Systems, South Korea), was used to measure applied normal force and surface roughness to analyze microscopic frictional measurements. Friction coefficients of the CoCr femoral head with boundary lubricants were calculated afterward.

Results

By using AFM techniques the surface roughness and frictional coefficient (μ) of the CoCr femoral head were measured at 12 different locations under the lubrication of PBS, BSA, and γ-globulin. The frictional coefficients of the CoCr femoral head in case of PBS decreased with increasing BSA concentrations. Statistically significant differences in μ were detected between the BSA concentration groups of 10, 20, 30 and 40 mg/ml, , though between the 30 and 40 mg/ml concentration groups were remain unspotted.

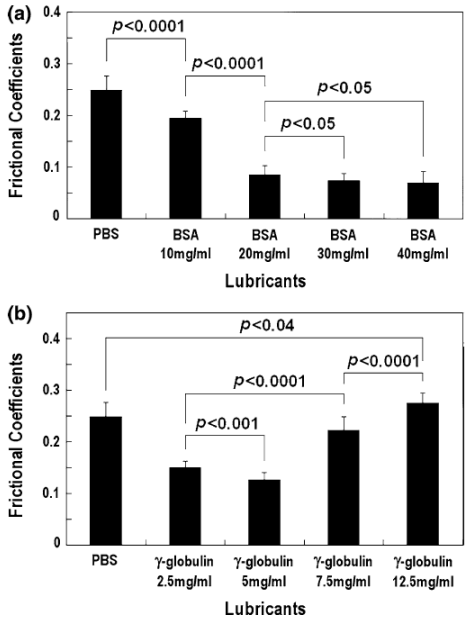

Fig. 12 AFM frictional coefficients of the CoCr femoral head measured in solutions of a PBS and BSA and b PBS and c-globulin from 12 different scanned areas at each concentration of the lubricants were presented as mean ± standard deviation values [16]

The concentration dependent change in μ was different from that with BSA while using γ-globulin as a lubricant at concentrations of 2.5 to 12.5 mg/ml, γ-globulin concentration decreased initially and then increased with decreased μ. Statistical differences in μ were significant between the γ-globulin concentration groups of 2.5, 5.0, 7.5, and 12.5 mg/ml in all cases and also between the PBS control group and any of the γ-globulin concentration groups (2.5–12.5 mg/ml).

Conclusions

Maximum level of BSA and optimal concentration of γ globulin leads to effective boundary lubrication. Thus the concentration of BSA and also γ globulin control the friction of CoCrMo head. These optimal concentrations of BSA and γ-globulin, can be utilized to increase the lubricating ability of CoCr hip prostheses by altering the surface roughness and coating materials of the bearing surface.

[12] **Park Jong-Bong, Cong-Truyen Duong, Ho-Geun Chang, Ashish R. Sharma, Mark S. Thompson, Sungchan Park, Byung-chan Kwak, Tae-Young Kim, Sang-Soo Lee & Seonghun Park,** "Role of hyaluronic acid and phospholipid in the lubrication of a cobalt–chromium head for total hip arthroplasty," *Biointerphases*, 9(3), 2014, 031007.

In this study boundary lubrication ability was determined for retrieved CoCrMo head within HA and PLs. Concentration dependent behaviour of HA and dipalmitoylphosphatidylcholine (DPPC) are revealed along with microscale frictional coefficients.

Materials and Methods

Retrieved CoCr femoral head was sectioned as a test sample with 10mm of length, 10mm of thickness, and 5mm of width from the main wear region and glued

to a cylindrical flat plate (1 mm thickness and 19mm diameter), and then fixed to a 50mm polystyrene petri dish with cyanoacrylate adhesive. Various concentrations of selected lubricants HA and DPPC and two control solutions PBS, (P5493, Sigma-Aldrich) and polypropylene glycol (PG, 438146, Sigma-Aldrich) were prepared. AFM (XE 70, Park Systems, South Korea) was used, including a rectangular silicon cantilever (NSC36-C, Micromash Inc.) integrated with sharp silicon tips. In contact mode at a scan frequency of 1 Hz surface scanning of 25 µm x 25 µm area with a resolution of 256 x 256 pixels was attained.

Results

When HA was dissolved in PBS as a lubricant, the concentration-dependent change in l of the retrieved CoCr femoral head was similar to that observed with DPPC. In the case of HA lubricant, the frictional coefficients decreased significantly at concentrations of 2.0 and 3.5 mg/ml while increased at 5.0 mg/ml, compared to that with PBS (0.25 $\pm$ 0.03).

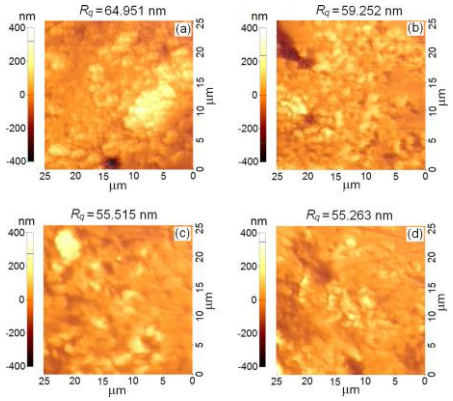

Fig. 13 Typical AFM images (2D) with a color scale in nm range of surface roughness (Rq) for the retrieved CoCr femoral head surface, taken over the scanned area of 25 lm_25 lm with a resolution of 256_265 pixels using sharp silicon tips, showing similar Rq values in different lubricants: (a) PBS, (b) HA 3.5 mg/ml, (c) PG, and (d) DPPC 0.2 mg/ml [12]

The concentration dependent lubrication behavior of DPPC was most effective when DPPC was in the physiological concentration range, showing µ=0.16 $\pm$ 0.01 in polypropylene glycol, and 0.05 $\pm$ 0.01, 0.02 $\pm$ 0.01, and 0.03 $\pm$ 0.01 at a DPPC concentration of 0.05, 0.2, and 3.0 mg/ml, respectively.

Conclusions

Retrieved CoCrMo head's The microscale frictional response has dependency on the concentration of HA and PLs. Optimal concentration that ranges to maximize frictional behaviour are similar to concentration of HA and DPPC of human synovial fluid.

[25] **Schmidt, Tannin A., Nicholas S. Gastelum, Quynhhoa T. Nguyen, Barbara L. Schumacher & Robert L. Sah,** "Boundary Lubrication of Articular Cartilage: Role of Synovial Fluid Constituents," *Arthritis & Rheumatology*, 56(3), 2007, 882-891.

This research is focused on contribution of boundary lubrication of various constituents of SF separately and also collectively. SF constituents HA, PRG4, and

SAPL graded concentrations and their differenent combination were utilized for cartilage boundary lubrication tests.

Materials and Methods

To determine the concentrations of HA the carbazole reaction for uronic acid, for PRG4 by enzyme-linked immunosorbent assay, and for PLs test phospholipid assay using PLs B standard solution and color reagent were used respectively. ELF 3200 (Bose EnduraTEC, Minnetonka, MN) equipment set up was used for the performance of cartilage boundary lubrication tests with fresh bovine osteochondral samples. Effect of graded dilutions was determined by the test lubricants prepared in PBS and different percentage of SF. Two friction coefficients (μ) were determined, to evaluate the boundary lubrication properties of test lubricants.

Results

Friction was modulated by test lubricant, in all experiments. Normal SF functioned as an effective boundary lubricant both at a concentration of 100% ($<\mu_{kinetic,\ Neq}>$ = 0.025) and at a 3-fold dilution ($<\mu_{kinetic,\ Neq}>$ = 0.029). Friction coefficients were reduced by HA and PRG4 in a dose-dependent manner. Thus both HA and PRG4 contributed independently to a low μ in a dose-dependent manner. In phosphate buffered saline Values of $<\mu_{kinetic,\ Neq}>$ decreased from ~0.24 to 0.12 in 3,300 μg/ml HA and 0.11 in 450 μg/ml PRG4. But in combination HA and PRG4 lowered μ further at the high concentrations, attaining a $<\mu_{kinetic,\ Neq}>$ value of 0.066.

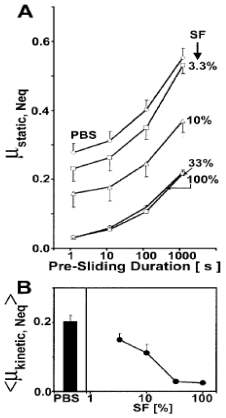

*Fig. 14 Effect of graded concentrations of synovial fluid (SF) on the boundary lubrication of articular cartilage. Shown are static ($\mu_{static,\ Neq}$) (**A**) and kinetic ($<\mu_{kinetic,\ Neq}>$) (**B**) friction coefficients in phosphate buffered saline (PBS) and various concentrations of SF. In **B,** the presliding duration was 1.2 seconds. Values are the mean and SEM (n = 4–8)* [25]

Friction coefficients were not affected by SAPL varied with test lubricant. SAPL at 200 μg/ml either independently or in combination with HA and PRG4 did not significantly lower μ.

Conclusions

Both at physiologic and pathophysiologic concentrations, constituents of SF contribute to the boundary lubrication of the apposing articular cartilage surface. The contribution found individually and also in combination of the constituents of SF.

[2] **Greene, G. W., X. Banquy, D. W. Lee, D. D. Lowrey, J. Yu A J & N. Israelachvili,** "Adaptive mechanically controlled lubrication mechanism found in articular joints," *Proceedings of the National Academy of Sciences*, 108 (13), 2011, 5255–5259 .

The research revealed frictional experiment on porcine cartilage and lubrication mechanism of enzymatic digestion of hyaluronic acid.

Materials and Methods

The cartilage samples collected from porcine knee articular joints were stored in Hank's buffer solution at −50 °C until use. Hyaluronidase (Sigma) was diluted with PBS buffer to a concentration of 200 units⁄mL then stored at −50 °C before use. Using surface force apparatus SFA 2000 equipped with friction device attachment normal and frictional force was measured under various loading conditions, with a friction device attachment or a 3D/XYZ device. The effect of enzymatic digestion of HA with hyaluronidese was investigated.

Results

HA with hyaluronidase on the dynamically changing and equilibrium friction forces in sheared cartilage against glass in PBS. This can be explained as an adaptive lubrication mechanism mediated by an interfacial HA-LUB complex layer. under different loading conditions this layer is regulated by the mechanical deformation response of the cartilage.

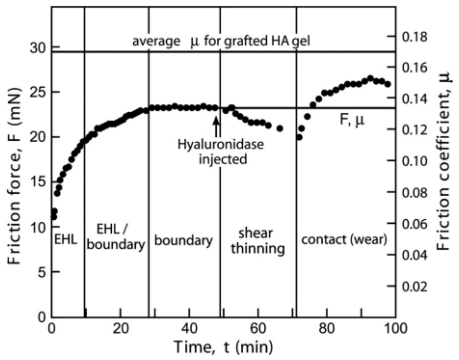

Fig. 15 The effect of HA digestion on the friction force between cartilage and glass in PBS [2]

As molecules of glycoprotein lubricin (LUB) and the interfacial HA layers at the cartilage surface are cross-linked and complexed with each other. In case of digestion of this layer also removes LUB molecules from the cartilage surface, afterwards removing the bulk of HA from the surface. This leads to decreasing the molecular weight of HA chains in the remaining layer.

Conclusions

It could be concluded from the experiment that hyaluronic acid and glycoprotein lubricin complex as HA-LUB, trapped at the interface to form a cross-linked network, which plays a role of boundary lubricant and prevent wear mechanism.

[26] **Nakashima Kazuhiro, Yoshinori Sawae, Teruo Murakami & Stefano Mischler,** "Behavior of Adsorbed Albumin Film on CoCrMo Alloy under In-situ Observation," *Tribology Online*, 10(2), 2015, 183-189.

This experiment covers the area of adsorption and frictional property of BSA in rubbing condition of ultra-high molecular weight polyethylene (UHMWPE) and

CoCrMo alloy. Electrochemical method was used to investigate *in-situ*, real time information on adsorption and desorption of proteins.

Materials and Methods

Reciprocating pin-on-disk tribo-meter with electrochemical cell was used to measure the potential and current measurement. Sliding pair were UHMWPE (GUR1050) pin specimen with spherical end of 10mm diameter and CoCrMo alloy (ASTM F75) disk with 5mm thick and 25 mm diameter functioned as work electrode. PBS with BSA 0.7, 1.4 and 2.1 mass% lubricants were used respectively to fill up electrochemical cell. Calomel reference probe was used as a reference prob to analyze the potential. Open circuit potential condition technique was used to cover friction force and electric potential. But -0.2 applied potential condition also measured electric current and friction force.

Results

Higher friction is observed with BSA 2.1 mass% and PBS compared with PBS solution. Thus BSA was adsorped on CoCrMo surface and midifies frictional coefficient high. A large drop after starting of rubbing was observed for BSA solution. Potential drop was smaller for PBS but the trasition was similar as BSA. PBS without protein has low friction. Whereas for protein higher concentration showed higher coefficient friction. As absorbed BSA films prevents direct contacts. The increase in potential for BSA solution expressed the amount of desorption under shear stress.

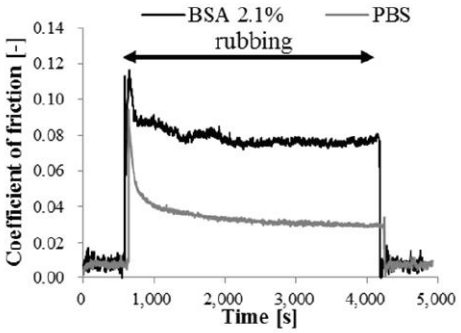

Fig. 16 The effect of friction transition under OCP condition [26]

Conclusions

Thus it is disclosed that BSA film is reconstructed during rubbing on CoCrMo alloy surface, under rubbing condition by shear force. Absorbed film formed become strong and stable and optimally adapted structure for shear force by receiving shear force.

[3] **Zhang, Z., S. Barman & G. F. Christopher,** "The role of protein content on the steady and oscillatory shear rheology of model synovial fluids," *Soft matter*, 10, 2014, 5965–5973.

Interfacial rheology and bulk rheology of model synovial fluid are focused parameters of this study, which are effect by the proteins and hyaluronic acid for respectively various shear rates, strains and frequencies.

Materials and Methods

A model synovial fluid was utilized for the experiment that contained HA-sodium salt (Sigma-Aldrich 53747), BSA (Sigma-Aldrich A3059), and γ globulin (Sigma-Aldrich G5009) dissolved in 10 mM phosphate buffered saline solution within pH 7.4. A double wall ring geometry and AR-G2 stress controlled TA instruments rheometer were used to measure interfacial rheology and bulk rheology respectively. During interfacial rheology measurement the applied frequencies and strains were set to match those of bulk experiments. In case of bulk rheology measurement solutions were characterized in both steady and oscillatory shear over a range of applied rates, strains and frequencies.

Results

In case of bulk aggregation of proteins or interaction between the HA and BSA, changed in geometry would not affect measured viscosity. Whereas, changing geometry to a 60 mm parallel plate decreasess this behavior, and using a single gap cup and bob geometry nearly negated as in the below figure.

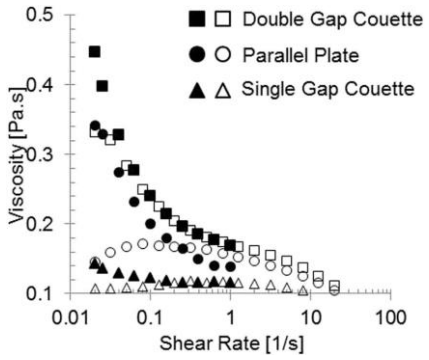

Fig. 17 Steady shear viscosities of model synovial fluid measured using 3 different geometries on a rotational rheometer [3]

A significant interfacial viscosity was observed in interfacial steady shear tests. BSA solutions showed remakable interfacial elasticity with moduli on the order of 0.01 Pa m in both strain amplitude and frequency sweeps in small amplitude oscillatory interfacial shear tests.

Conclusions

In steady and oscillatory condition of model synovial fluid composed of HA, BSA and γ-globulin interfacial rheology occured due to protein adsorption at the interface are rejected. On the contrary, bulk rheology was controlled wholly by HA of model SF in difference of shear rate, strains and frequencies.

3.3 Biochemical composition of Synovial Joint contents

Below researches are concentrated with the biochemical compositions synovial joints, where in most cases spectroscopic technique was used as an analyzing tool.

[20] **Jemma G. Kerns, Panagiotis D. Gikas, Kevin Buckley, Adam Shepperd, Helen L. Birch, Ian McCarthy, Jonathan Miles, Timothy W. R. Briggs, Richard Keen, Anthony W. Parker, Pavel Matousek, and Allen E. Goodship,** "Evidence from raman spectroscopy of a putative link between inherent bone matrix

chemistry and degenerative joint disease," *Arthritis & Rheumatology,* 66 (5), 2014, 1237–1246.

By using Raman spectroscopic technique, differences of molecular structures between tibial plateaus of respectively healthy joints and joints with total replacements due to osteoarthritis were compared. Also, comparison of medial and adjacent compartments of subchondral bones were observed as different load baring sites.

Materials and Methods

Different Tibial plateaus where collected from patients undergoing total knee replacement for OA (n = 10), from healthy joints from patients undergoing leg amputation (n = 5; sex- and laterality-matched) and from non-OA cadaveric knee specimens (n =5; agematched). To analyze volumetric bone mineral density and thickness of the subchondral bone the medial and lateral compartments of the tibial plateaus were scanned using pQCT (XCT 3000; Stratec). InVia Raman microspectrometer (Renishaw) equipped with an 830-nm laser, 300 mW was used to determine the molecular structural change occurrence in subchondral bone matrix.

Results

While detemining the density it was found that the OA tibial plateaus has significantly higher density across compared to the non-OA samples of the subchondral bone. Whereas comparing the tibial compartments, the medial sub-chondral bone had a significantly higher structural density than the lateral subchondral bone. Principal components analysis from raman spectral signature revealed a large separation of spectra (confidence interval 0.95) between the non-OA and OA specimens. Although, between the medial and lateral compartments within each cohort there was no difference observed.

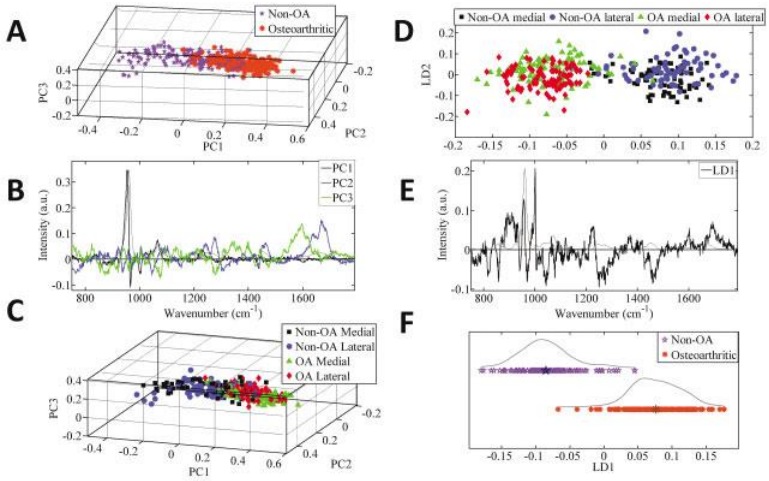

Fig. 18 Principal components analysis (PCA) of the Raman spectra. ***A–C,*** *Plot of PCA scores for the non-osteoarthritis (non-OA) tibial specimens compared to the OA tibial specimens* ***D–F,*** *Plot of PCA–linear discriminant analysis (PCA-LDA) scores for the non-OA and OA medial and lateral compartments [20]*

Conclusions

There was a huge remarkable difference observed between the profiles of the non-OA and OA specimens. Specifically tibial plateaus of medial and lateral for both bone matrix significant chemical structural changes appear due to OA. Whereas spectral differences were not found between medial and lateral compartment of the subchondral bone matrix.

[11] **Galandáková Adéla, Jitka Ulrichová, Kateřina Langová, Adéla Hanáková, Martin Vrbka, Martin Hartl & Jiri Gallo,** "Characteristics of synovial fluid required for optimization of lubrication fluid for biotribological experiments," *Journal of Biomedical Materials Research Part B: Applied Biomaterials*, 105(6), 2017, 1422-1431.

This study covers with the analysis of differences of the compositions and the constituents of synovial fluid extracted from respectively patients of primary arthroplasties and revision arthroplasties and without joint replacement and healthy synovial fluids.

Materials and Methods

Synovial fluid collected from 152 patients were categorized into four different groups depending on their conditions of OA and TJR. Group I were the patients with aseptic loosening of TJR; Group II had patients with TJR but without any signs of aseptic loosening and/or periprosthetic osteolysis; Group III were patients without TJR and with end-stage osteoarthritis; and Group IV had patients without TJR, without OA, and with non-inflammatory SF.

The total protein, albumin, and γ-globulin concentrations in SF were analyzed for each group. Reaction accompanied by the reduction of Cu^{2+} to Cu^{+} by the protein and formation of a colored complex proteins concentration were detected. Quantitative colorimetric kit, Enzyme-linked immunosorbent assay and Vibro-viscometer SV-1A were used respectively to determine concentration of PLs, HA and viscosity of SF. For statistical analysis IBM SPSS Statistics 22 software was used.

Results

Results of the concentrations of SF contents and viscosity are given in the following chart. The volume of SF in group I was significantly lower compared with that in group III and group IV. Similarly, SF volume in group II was significantly lower compared with group III and group IV.

Table. 2 Biochemical and Flow Parameters Detected in Different Groups of Joint Fluid Samples [11]

	Group I	Group II	Group III	Group IV
Volume of SF (mL)	2.5 (2.0–3.8)[a]	2.8 (1.8–9.3)[b]	11.0 (7.3–15.0)	12.0 (8.6–13.0)
Total protein (mg/mL)	40.3 (33.1–44.0)	39.1 (33.3–42.5)	35.5 (29.9–41.8)	37.9 (31.0–50.1)
Albumin (mg/mL)	28.2 (21.2–31.6)	27.9 (22.7–32.3)	26.7 (22.6–33.6)	29.1 (19.1–37.2)
γ-globulin (mg/mL)	11.5 (9.1–13.3)	10.5 (8.7–12.5)	8.7 (6.8–11.1)[c]	10.2 (6.8–13.5)
HA (mg/mL)	1.4 (0.4–2.8)	0.8 (0.5–1.5)	1.9 (1.0–3.5)	2.0 (0.8–3.4)
PLs (mg/mL)	0.154 (0.038–0.306)	0.175 (0.073–0.256)	0.305 (0.171–0.552)[d]	0.312 (0.125–0.513)
Viscosity (mPa/s)	54.3 (1.5–169.0)	54.0 (7.2–267.5)	61.8 (8.0–171.0)	7.3 (3.6–60.7)

The values are expressed as the median (the first quartile–the third quartile). Group I: Patients with aseptic loosening of TJR. Group II: Patients with TJR but without any signs of aseptic loosening and/or periprosthetic osteolysis. Group III: Patients without TJR and with the end-stage of osteoarthritis. Group IV: Patients without TJR, without osteoarthritis, with non-inflammatory SF.

[a] Significantly different *versus* group III ($p < 0.0001$) and IV ($p < 0.0001$).

[b] Significantly different *versus* group III ($p = 0.0001$) and IV ($p = 0.0002$).

[c] Significantly different *versus* group I ($p = 0.021$).

[d] Significantly different *versus* group I ($p = 0.019$) and II ($p = 0.012$).

SF, synovial fluid; HA, hyaluronic acid; PLs, phospholipids.

γ-globulin concentrations varies between group I and group III. Data for aseptically failed total hip and knee arthroplasty showed there are no difference in terms of concentration of PLs and HA. . No remarkable difference was obseved in the total protein content, albumin concentration and viscosity among the groups.

Conclusions

Therefore, albumin and γ globulin readily adsorbed on artificial materials, whereby have an influence on the frictional properties of lubricating surface. The γ-globulin concentration found remarkably higher and concentration of Pls observed significantly lower with revision of joint replacement patients and with patients without joint replacements. HA and viscosity of different groups were observed unchanged.

[13] **Esmonde-White Karen A., Gurjit S. Mandair, Farhang Raaii, Jon A. Jacobson, Bruce S. Miller, Andrew G. Urquhart, Blake J. Roessler A Michael D. Morris,** "Raman spectroscopy of synovial fluid as a tool for diagnosing osteoarthritis," *Journal of biomedical optics*, 14(3), 2009, 034013.

This paper presents investigation of differences between biochemical compositions of healthy joint synovial fluids and synovial fluids of OA patients.

Materials and Methods

The evaluation was enrolled for 40 patients with clinical evidence of chronic knee pain and patients scheduled for elective surgical treatment. To assess symptomatic knee pre-operative conventional postero-antero radiographs of the pateints were reviewed. From knee joint radiographic severity Kellgren/Lawrence (K/L) scores were used, for grouping individual patients. Drop deposition/Raman Spectroscopy protocol (DDRS) was utilized as an evaluation tool to distinguish between OA patients' SF and healthy joint SF. Light microscope was used for coarse separation from dried drop.

Results

From DDRS the dried drop contains two distinct regions, a glassy appearance of outer edge and center with fern shaped crystalline deposits and also some radial cracks along the edges. Primarily protein raman bands are visible from spectra of drop edges. The remarkable differences between no damage and damage groups are

ratios 1080 cm^{-1}/1001 cm^{-1} and amide I band intensity ratios, respectively which are sorted by K/L score. This ratio increases in the damage group, that characterized the chemical environment of the protein backbone is changing with OA damage. Disorder in protein secondary structure provide further evidence of altered electrostatic interactions.

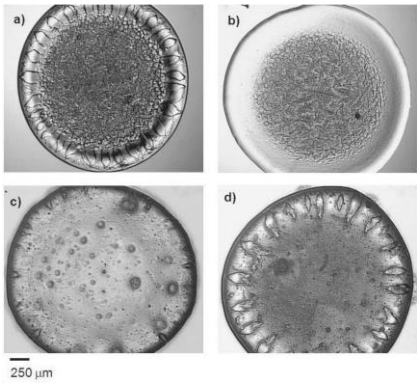

Fig. 19 Microscope images of human SF dried drops at low magnification show a heterogeneous deposit [13]

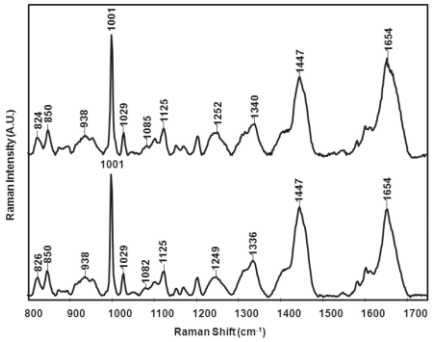

Fig. 20 Raman spectra collected from SF drop edges contains bands that convey chemical and structural information [13]

Conclusions

Thus DDRS method can be used as an appropriate detector of synovial SF of osteoarthritis patients, namely the raman band describes protein secondary structure. Raman data clarified that disorder within normal electrostatic interactions of SF occurs due to OA.

3.4

3.4 Usage of Raman Spectroscopy to evaluate Synovial Joint Replacement

The research area of SF and synovial joint replacement has been expanded with the imposition of raman spectroscopic technique. In below studies the raman data evaluation on this ground has been discussed.

[27] **Zhu Wenliang, Elia Marin, Nobuhiko Sugano, & Guiseppe Pezzotti,** "Tensor-resolved Raman spectroscopic analysis of wear-induced residual stress fields in long-term alumina hip-joint retrievals," *Journal of the mechanical behavior of biomedical materials*, 66, 2017, 201-210.

This is a research of polarized raman analysis of wear-induced (residual) stress fields on two different long-term alumina ceramic hip femoral retrievals working against polyethylene liners. There is also an analysis of evolution of tensor-resolved residual stress motifs in the three-dimensional space.

Materials and Methods

Two alumina hip femoral retrievals of 28 mm sized head referred as Case I and Case II were investigated, both were slid against polyethylene (PE) liners. Case I followed by bilateral hip OA secondary to developmental dysplasia of the hip treated with cementless Lubeck system. Case II the observation comprised with alumina ceramic femoral slid against the PE liner with a metallic wire marker. Where the ceramic bearing surface directly slid against the metallic back-holder. Raman spectra of these samples were obtained at room temperature while using a triple monochromator (T-64000, Jobin-Ivon/Horiba Group, Kyoto, Japan) equipped with a charge-coupled device (CCD) detector. A back-scattered confocal laser microscope (Keyence, VK-X210, Osaka, Japan) were used to determine the optical morphologies of the samples.

Results

The microstructure of the Al_2O_3 heads surface in the main wear (MW) and non-wear (NW) zones were analyzed under the laser microscope. It was found a coarse grain structure (especially for Case II, grain size > 10 μm) and extensive grain pullout throughout the head surface.

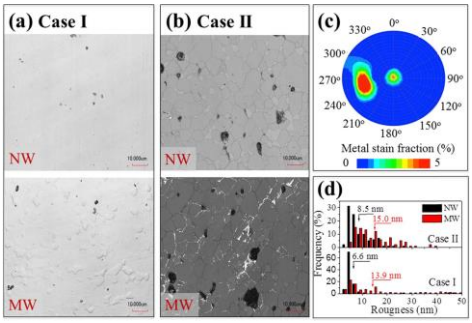

Fig. 21 Microstructures of the Al2O3 heads in MW and NW zones of (a) Case I and (b) Case II, as observed by laser scanning microscopy; (c) polar map of the main wear zone of Case II (d) histograms of surface roughness in MWZ and NWZ of the two Al2O3 heads [27]

Polarized raman spectra of implanted Al_2O_3 femoral heads were observed in MWZ of the bearing surface of the both Al_2O_3 retrievals in parallel polarization configurations. At room temperature, α-Al_2O_3 possesses a structure belonging to the 3*m*(*D*3*d*) point group and shows 7 Raman active bands, including two A_{1g} modes and five E_g modes.

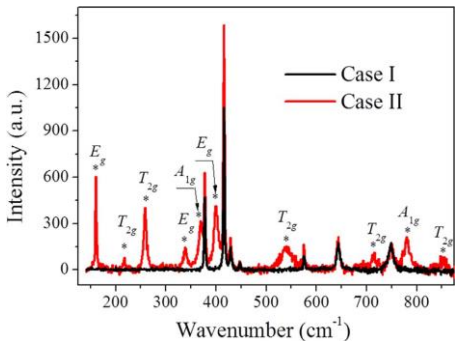

Fig. 22 Typical Raman spectra collected on the alumina heads [27]

Conclusions

On the ceramic surface of the two femoral heads a remarkable difference in the residual stress field stored was found. The evolution of residual stress motifs in space including exceptionally high shear stresses in one case, were revealed. The micromechanical features linked with joint performance that occur in real in vivo condition could be uncovered by this developments of raman spectroscopic algorithms.

[21] **Taddei Paola, Modena Enrico, Traina Francesco & Saverio Affatato**,"Raman and fluorescence investigations on retrieved Biolox® delta femoral heads," *Journal of Raman Spectroscopy*, 43(12), 2012, 1868-1876.

The molecular level characterization of BIOLOX®delta retrievals was the purpose of the study. Fluorescence and raman spectroscopic technique were used to obtain the results showed material properties alteration of BIOLOX®delta femoral heads.

Materials and Methods

From six different patients who underwent primary total hip arthroplasty of six retrieved BIOLOX®delta (CeramTec AG, Plochingen, Germany) femoral heads were collected. The retrievals were BIOLOX®delta-on- BIOLOX®delta hip joints replacement as summarized in below Table.

Table. 3 Details on the BIOLOX® delta *retrievals analysed in the present study [21]*

Case	Implant year	Gender	Side of implant	Age (years)	Follow-up (years)	Weight (kg)
#1	1999	F	SN	77	8	78
#2	2003	F	SN	48	5	57
#3	2006	F	SN	78	3	85
#4	2007	F	DX	67	2	60
#5	2009	F	DX	85	1	78
#6	2009	M	DX	80	1 month	73

A Jasco NRS-2000C micro-raman spectrometer was utilized equipped with a 160 K frozen digital charge-coupled device. Micro-raman spectra were obtained using an argon laser operating at 514 nm. By raman and fluorescence spectroscopy six fragments of the head were analysed in their fractured sections. Also new BIOLOX®

delta femoral head was coupled with a homologous acetabular cup and the bearing was run into a hip joint simulator for $1x10^5$ cycles without lubrication was analysed for comparison.

Results

The average micro-Raman spectra of two representative retrievals, #2 and #4 were presented here through the spectra recorded on both unworn control (black) and worn (red) areas. In the unworn region of the retrieval #2 raman spectrum observed the marker bands of tetragonal zirconia at 648, 464, 317, 268 and 147 cm^{-1} together with those assignable to the monoclinic polymorph at 627, 577, 541, 506, 481, 382, 338, 227, 191 and 182 cm^{-1}.

The monoclinic volume fraction Vm = 0.42±0.03 was calculated from the spectral features at 147 and 191–182 cm^{-1}, in the unworn area of retrieval #2. Significantly lower Vm contents observed in retrieval #4 in both unworn and worn regions, which was more recently implanted. The fluorescence spectrum of a BIOLOX®delta component was observed fitted into the two R1 and R2 components. The intensity of these bands was more postulated than in pure alumina because of the presence of chromium in the BIOLOX®delta formulation.

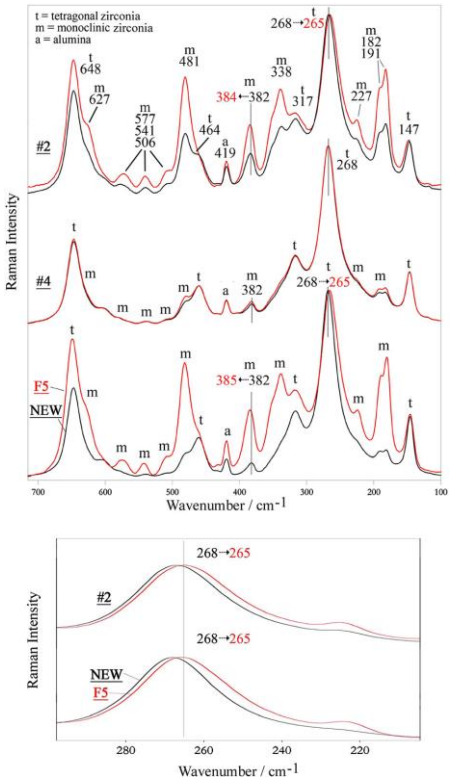

Fig. 23 Average micro-Raman spectra recorded on some representative BIOLOX®delta femoral heads [21]

Conclusions

A progressive improvement of the material properties occurrence in the period comprised between 1999 and 2009 is proved by fluorescence and raman. Also the spectroscopy proved tetragonal-to-monoclinic t zirconia ransformation occurence

is due to wear. It was found that the mechanism operating in vivo was found to be the same active in vitro, as that can simulate the effect if in vivo wear.

[28] **Choudhury Dipankar, Matus Ranuša, Robert A. Fleming, Martin Vrbka, Ivan Křupka, Matthew G. Teeter, Josh Goss & Min Zou**,"Mechanical Wear and Oxidative Degradation Analysis of Retrieved Ultra High Molecular Weight Polyethylene Acetabular Cups," *Journal of the Mechanical Behavior of Biomedical Materials*, 2018.

Ten retrieved and four new mildly cross-linked ultra-high molecular weight polyethylene (UHMWPE) acetabular liners were analyzed in terms of surface deviation, oxidative degradation and changes in material properties.

Materials and Methods

Techniques used for the measurements of this experiments were respectively micro-computed tomography (micro-CT) scan, 3D laser scanning microscopy, raman spectroscopy and nanoindentation. To characterize the microstructures of the UHMWPE liners in terms of variation in the orthorhombic crystalline phase fraction and oxidation indices the utilized equipment was confocal raman microscope (inVia™, Renishaw). A schematic view of such measurement is shown in the Figure total of nine (9) points on each liner were measured.

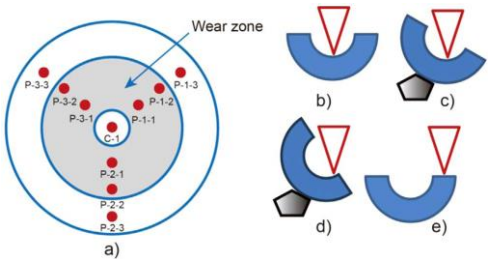

Fig. 24 The schematic diagram for confocal Raman (non-destructive) assessments of oxidation index in UHMWPE for the locations of measuring spots [28]

Finally an instrumented nanoindenter was used to measure the hardness and modulus of elasticity.

Results

The mapped surface deviation spectra across the acetabular liners have positive values indicates material inflation and negative values indicates penetration (wear/creep) on the retrieved liners. Interestingly, most of the wear/creep areas were eccentric but a few were centric.

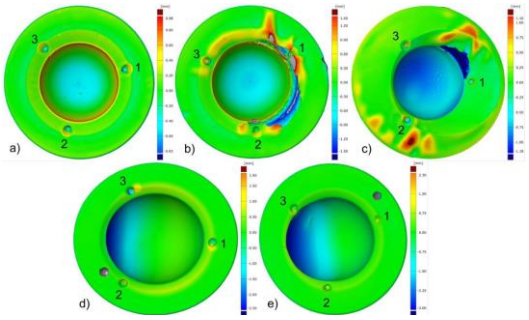

Fig. 25 Mapped surface deviation (mm): (a) sample 1, (b) sample 2, (c) sample 3, (d) sample 4 and (e) sample 5. Positive values refer to material inflation and negative values refer to material wear [28]

Samples with centric wear area had higher surface roughness compared to the samples with ecentric wear area. But in case of few samples had eccentric wear but exhibited one the rougher surface follwed by failure mechanisms.

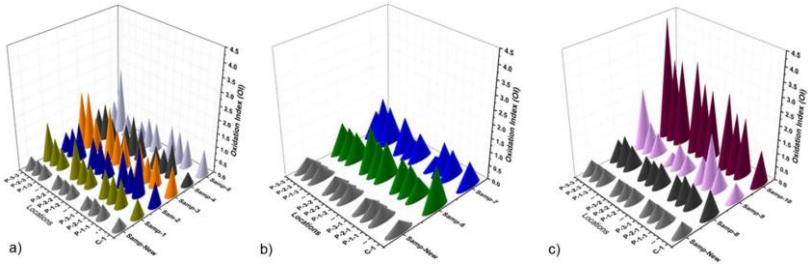

Fig. 26 Oxidation index for the retrieved samples: (a) group 1, (b) group 2, and (c) group 3 [26]

The oxidation indices were measured and found that for all retrieved samples have higher oxidation indices at the contacting side wall and the rim regions compared to that of a new sample.

Conclusions

Chemical degradation were identified in the retrieved prosthesis through the oxidation indices. One of the most denominating factor was eccentrically worn track for higher penetration rate. Also material inflations were found in few samples rim areas and contact areas. Ultimately hardening and stiffening were observed in these analyzed prostheses.

4 ANALYSIS, INTERPRETATION AND EVALUATION OF FINDINGS OBTAINED FROM CRITICAL REVIEW

Inflammation is a highly regulated process, tightly linked to simultaneous stimulation of tissue protective and regenerative mechanisms in order to prevent collateral damage of peri prosthetic tissues. A variety of cytokines, chemokines, hormones and specific cell populations, including macrophages, dendritic and stem cells, attempt to balance tissue architecture and minimize inflammation.

While determining specimens protein, PLs and HA contents of joint fluid samples obtained from patients undergoing total knee arthroplasty (TKA) and revision TKA, it is found that even though the total protein content was normal, the specific proteins present in these diseased joints may have differed from those present in healthy joints. The bulk properties of the fluid may control fluid film lubrication as Mazzuccoa et al.[14] stated that, there would be some connections between the composition of joint fluid and the tribology of joint replacement prostheses in vivo.

Patient synovial fluid chemistry plays an important role in determining implant wear and the likelihood of failure [4].

From the experiment of Galandakova et al.[11] it is shown that The γ-globulin concentration was significantly higher and the PLs concentration significantly lower in patients with revision of TJR compared with patients without TJR. No significant difference was found in HA concentration and viscosity among the groups.

There is a maximum concentration for BSA to act as an effective boundary lubricant. One the other hand the lubricating ability of γ-globulin is most effective in the physiological concentration range within human SF. BSA with the alfa-helix structure provides low adsorption strength between its protein and the bearing surface, while γ-globulin with the βsheet structure has a tendency to adsorb strongly on the rubbing surfaces and yields large cohesive and/or adhesive forces on the bearing surface in a mixed or boundary lubrication regime. This difference of adsorption strengths between BSA and γ-globulin could be responsible for a difference in the concentration-dependent lubricating ability between them [16].

Since the human body composed of a highly corrosive environment, very stringent requirements are imputed on the candidate materials' properties [29].

Optimal concentration of HA and PLs, DPPC for effective lubrication is similar to that observed in normal human synovial fluid. The microscale frictional response of the retrieved CoCr femoral head has a significant dependence on the concentrations of HA and DPPC [12]. In arthritis, injury, and artificial joint failure, there is increased friction between the articulating surfaces and concomitant erosion of the load bearing elements [7, 30].

Minor variations in test solution chemistries can significantly influence to the wear–corrosion behaviour of the cast CoCrMo alloy. CoCrMo is reported to be susceptible to corrosion when implanted into the human body (pH 7.4), especially within a tribological contact such as a knee or hip [31]. The initial corrosion products

occurred when the passive film is damaged are reported to be Co^{2+} and Cr^{2+} species in acidic conditions and CoO and CrO at neutral pH, respectively [31, 32]. Films formed from protein solutions dependent on the protein content and solution pH [22, 24].

Buffer choice affects protein film formation in static and rolling conditions. Solution pH dominates both the protein adsorption kinetics and the formation of tribofilms in static and rolling conditions respectively. The aspect of the buffer which had the dominant effect on static adsorption was pH. The rate of protein adsorption, as well as the viscoelastic properties of adsorbed layers for all buffer chemistries is similar, the slight differences being within experimental error. That is for the solutions tested the buffer chemistry makes no significant changes to protein adsorption [24].

According to boundary lubrication mechanism, proteins adsorb at the CrCoMo surface to form thin, discontinuous deposited films. Wear mechanisms are primarily driven by tribocorrosion processes: Increasing pH increases CoCrMo wear [4].
The component concentration, particularly for the proteins, can vary greatly [5]. Diseased and periprosthetic synovial fluid undergoes changes including decreased effective viscosity, increased protein content and increased pH [4, 5].

Toshio et al.[5] stated that the presence of albumin in the lubricant promotes pH dependence and viscosity independence of the tribological properties at low speed. While the presence of globulin promotes pH and viscosity independence at low speed and promotes pH and viscosity dependence at high speed in the lubrication of ultra-high molecular weight polyethylene (UHMWPE) against stainless steel (SUS). The effect of constituents and pH changes in periprosthetic fluid for the lubrication is a clue toward resolving many complications after total joint replacement.

Significant influence of the composition of the electrolyte in the passivation behaviour of Co-based alloys is been observed several times. The adsorption of organic species present in the synovial fluids assumed as attach with this passive film and modifies their surface reactions. Protein adsorption onto metallic surfaces affects the biocompatibility of the biomaterials since, an accelerated metal dissolution may be favoured. On the other hand, it has been found that the presence of a biofilm on the surface formed by protein or amino acids can act as a lubricant film reducing friction, hence reducing mass lost [33, 34]. But it is yet to be clarify the chemistry is held with the biofilm.

High-concentration protein fluids form an inlet reservoir of viscous material that is entrained into the contact forming a separating film. The organic deposits reported in the literature on implant surfaces are formed by agglomerated-proteins. In the fluid environment these deposits are viscous and can be easily removed by surface scratches. Once removed from the fluid they dry to form highly-adherent, solid films [4]. Therefore chemical structure of the solid film is to be understandable.

From the study of Fan et al. [4] it was also stated that when γ-globulin was present much thicker films were measured and also a thin residual film is formed by mono or

multilayer adsorbed protein molecules. If the chemistry of formed film of γ-globulin is analyzed separately, most likely, that can provide an interesting result.

It is also stated that under rolling, protein layers are much thicker than statically adsorbed layers [22].

While Nakashima et al. [26] observed Friction force and electric potential were measured under open circuit potential OCP condition in the rubbing combination of UHMWPE and CoCrMo alloy, the adsorption behavior of BSA showed the desorption at first rubbing, and gradual decrease in desorption amount. BSA film on metal surface under rubbing condition is reconstructed during rubbing and the adsorbed film formed during rubbing is stable and has an optimally-adapted structure for shear force and can sustain its property during rubbing.

The role of proteins on the electrochemical behaviour of bio-metallic surfaces is the aspect to comprehended [33]. Thus resolving this unknown area of the chemistry of the biofilm could be very significant in this research field.

From above discussion it is shown that the film formation on the joint replacement is dependent on pH concentration and viscosity of the solution, but the chemical composition of the formed film still remains unknown.

5 ESSENCE AND GOALS OF THE PH.D. THESIS

The research aims to clarify the chemistry of SF components due to the film formation of joint replacement along with the film's mechanical properties. It is visible from the above discussion that the formation of the film is dependent on various parameters, such as pH of the solution and static and rolling conditions, viscosity and concentration of the solution, which are already revealed. Thus, it is high time to detect the occurrence of the chemical change of SF, for the proper understanding of the condition of joint replacement and further improvement of the durability of the replaced area. Raman spectroscopy is a unique technique to explain the biochemical behavior of the materials using in joint replacement. Therefore, chemical analysis, including the study of mechanical and biological properties of the SF of joint replacement, will improve the concept of the process.

Due to the different biological components' existence within the SF, the characteristics of formed films are dependent on the variety of SF protein and other constituents. Depending on the chemical composition of these components, the chemical nature of films could also differ. The main goal of this research is to obtain the chemical reactions occurring within the joint replacement, along with the frictional coefficient measurement. It is considered the combination of the chemical reaction and frictional coefficient within artificial joint replacement may reveal some reality, to uncover more practical results to realize the lubrication chemistry and mechanism of SF within the prosthesis.

6 SCIENTIFIC QUESTION AND WORKING HYPOTHESIS

Scientific question:

Which components of SFs are adsorbing chemically while lubricant film formation on hip implant material surfaces within artificial joint replacement?

What kind of chemical structural changes are taking place within the constituents of SF in hip prosthesis and how frictional coefficients are differing with this chemical change?

Working hypothesis:

The principal causes of OA are assumed to be classified into two main classes. The first one is a change of the chemical composition of the bone matrix as well as the SF. Most likely, the secondary structures of SF proteins and tropocollagen are affected in osteoarthritis. The other one could be articulated as the mechanical loading change, which leads to the total joint replacement of patients due to the stiffer structure. [11, 20, 13].

1. **Change of Chemical composition**

Esmondewhite et al. [13] considered the change of chemical structure within SF under OA and total joint replacements and concluded that differences occurred in diseased SF compared to healthy SF. Besides, Jemma Kerns et al. [20] confirmed that the subchondral bone matrix also altered its chemical structure due to OA. Both above observations of chemical structural changes were investigated through Raman spectroscopy. Nevertheless, the structural changes of individual components of synovial fluid must be addressed to understand these chemical changes thoroughly. To observe the biochemical reactivity of the SF on the implant materials, the usage of different synovial components in appropriate ratios may show more realistic results to understand the lubrication chemistry and mechanism of SF within the replaced joint. Raman Spectroscopy could be the most suitable technique to explain the biochemical behavior of SF and its components as well as the implant materials using in joint replacement.

2. **Mechanical loading change**

Most of the studies found are concerned with adsorption and desorption of proteins in different kinematic conditions and film thickness in different pH, buffer and concentration of proteins [15, 22, 26, 23, 24, 4, 25]. Frictional coefficients, frictional force, shear force, wear measurement, boundary lubrication, surface geometry, rheology of various constituents are also considered with proteins and other SF components to explore the knowledge in this area [2, 3, 16, 26, 10, 12, 25]. To take into account the mechanical and chemical environment of human synovial joint, viscosity of various modal fluids and wettability of various surface materials were also considered [10-12, 23, 24] concerning their duration in time and under varying temperature and pressure [2, 23]. Therefore in this present condition, it is essential to consider the change of mechanical properties sequentially along with the

chemical change to visualize the whole picture of alteration of the environment of the synovial joint after replacement.

Thus in this study, the sought-for information would be the chemical composition of synovial fluid film through simultaneous consideration of mechanical properties such as frictional coefficient within the control of temperature and pressure. The Aim would be to obtain the correlation of coefficient of friction of each experimental set of SF liquids and implant materials.

7 METHODS

7.1 Material

7.1.1 Pendulum hip simulator

The Pendulum hip simulator is explained as an unprecedented and unique bio-tribological instrumentation that replicates 'flexion and extension' of artificial hip joints condition, alongside their real geometry, body temperature and load. It is also capable of measuring a real-time velocity profile, average friction coefficients and a viscous effect(an indicator of lubrication film formation). Vrbka et al. conducted his experiment with this mechanism to visualize lubricating films between artificial head and cup concerning real geometry and Necas et al. also utilize the same to understand the effect of diameter, clearance and material of in situ observation of lubricant film formation.

Dipankar et al. used this simulator to understand a significant friction coefficient reduction to the 'dimpled a-C:H/ceramic' prosthesis compared to a 'Metal(CoCr)/ ceramic' prosthesis. As a result, it is indicated that the simulator can be utilized as an advanced bio-tribometer. [35, 36, 37]. Based on the principles of the pendulum hip joint simulator was used as a test device for film thickness measurement by an optical imaging system.

The simulator is composed of a base frame with the acetabular cup and the swinging pendulum with the femoral head. Electromagnetic motors are employed to drive the pendulum allowing a continuous motion in the flexion−extension plane [37].

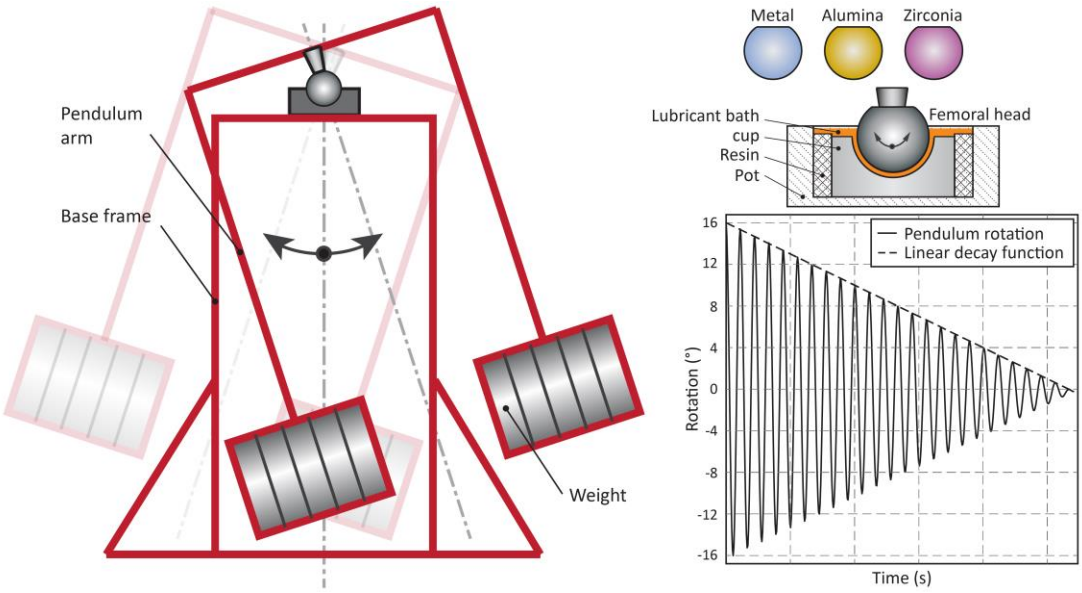

Fig. 27 Schematic diagram of Pendulum hip simulator [38]

The coefficient of Friction for several contact pairs were determined within the pendulum hip joint simulator. The acetabular cup is installed by resin in a stainless-steel pot. This set up is mounted to the base frame. The swinging arm using a cone is connected to the head. When the experiment starts, the pendulum arm is deflected to the primary position and then released. Between the ball and the cup, the impulsive swinging is then damped due to friction. Instant deflection of the pendulum is recorded via an angular velocity sensor. Consequently, the processed signal is enclosing to obtain the friction coefficient. A linear model of damping is utilized for evaluation [38].

It is supposed that this kind of instrument set up could be helpful for determining the chemical reaction within synovial fluid after artificial joint replacement along with the frictional coefficient of each contact pair.

7.1.2

7.1.2 Ball-on-cup configuration

While clarifying the lubrication processes within artificial joints considering the ceramic femoral heads were focusing on the role of particular proteins, by Necas et al. The experiments were conducted in a ball-on-cup configuration, where the contact couple was the ball made from ceramic and the acetabular cup from glass. The measurements were conducted using colorimetric interferometry and fluorescent microscopy under pure rolling, partial negative and partial positive sliding [19].

While clarifying the lubrication processes considering within artificial joints this experiment would be conducted in a ball-on-cup configuration. The first contact couple would be the ball made from CoCrMo and the acetabular cup from polyethylene or glass. Thus, for this experiment to explain the effect of tribology, metal hip prosthesis head of CoCrMo ball (28mm) from Zimmer would be used as per ISO 5832-12, which contains metal as cobalt-chromium casting alloy. The cup would be used made from polyethylene from Smith and Nephew 28mm and tailor-made acetabular cup from optical glass (BK7).

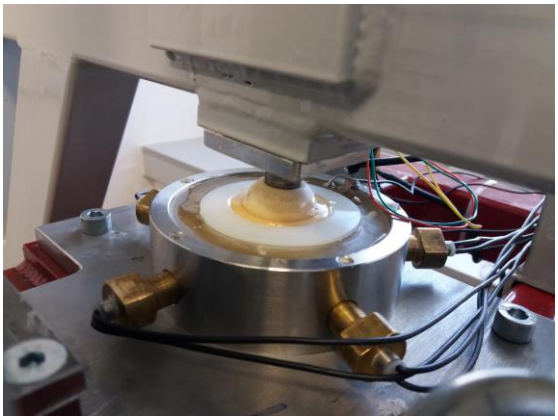

Fig. 28 Ball on cup configuration in Pendulum hip simulator

The other two ball-on-cup sets are made from two types of ceramics. Alumina ceramic ball would be used that is BIOLOX®forte from Zimmer- sulox (28mm), and the cup of the same component would be used from smith and nephew. And the set of ball and cup is of zirconia toughened alumina ceramic to be precise BIOLOX®delta (28mm), and the cup would also be made from the same component. Both ball and cup of BIOLOX®delta are used from Zimmer.

7.1.3 Model fluid Lubricants

Within hip replacement to observe the chemical reaction occurs, three types of model SFs would be used as lubricants within the ball on cup configuration. These model fluid were prepared according to the concentration of the components of real physiological SFs evaluated by Galandakova et al. [11]. The types of model fluids used here are respectively the mimic of SF of healthy or physiologic joint (SF1), SF of total joint replacement (SF2) and SF within a joint with osteoarthritis (SF3) [11, 39]. In the model fluids, the concentration of albumin, γ-globulin, HA and phospholipid were maintained within the range of the situation of human joints described in Table 4.

Table 4: Composition and concentration of the applied test lubricants.

Test Fluid	Albumin *(mg/ml)*	γ-globulin *(mg/ml)*	Hyaluronic Acid *(mg/ml)*	Phospholipid *(mg/ml)*
Albumin	28	-	-	-
γ-globulin	-	11	-	-
Hyaluronic Acid (HA)	-	-	2	-
Healthy Joint (SF1)	20	3.6	2.5	0.15
After Total Joint Replacement (SF2)	26.3	8.2	0.87	0.35
Joint with Osteoarthritis (SF3)	24.9	6.1	1.49	0.34

Albumin, γ globulin, HA and phospholipid will be dissolved in PBS, which will be used as the base fluid, for overnight at 4^{o}c while employing laboratory rocker-shaker (MR-12, Biosan, Riga, Latvia). The next step of preparation is mixing each of the individual components' solutions in the same solution in order albumin, γ-globulin, HA, phospholipid. The product specifications of the components applied are as stated here. Bovine serum albumin (powder, ≥96%; A2153, Sigma-Aldrich, St. Louis, MO, USA), γ-globulin from bovine blood (powder, ≥99%; G5009, Sigma-Aldrich, St. Louis, MO, USA), HA = Sodium Hyaluronate HySilk (powder, quality class—cosmetic; molecular weight = 820–1020 kDa, Contipro, Dolní Dobrouc, Czech Republic), and PHs = L-α-Phosphatidylcholine (powder, Type XVI-E, lyophilized

powder; ≥99%; vesicles form; P3556, Sigma-Aldrich, St. Louis, MO, USA). Lubricant solutions will be preserved in -22^{o}c after preparation.

Albumin (28.0 mg/ml), γ-globulin (11.0 mg/ml) and HA (2.0 mg/ml) amd 25% BSA would be tested separately to observe the chemical reaction occurring on implant surfaces.

The pendulum hip joint simulator set up 5-6 mins to observe the tribological effect of each of the lubricants to obtain the chemical impact on the ball surface. The lubricants will be collected from the cup after tribological tests for analysis. The temperature will mainatain 37 ^{o}c throughout all the experiments and 15kg weight would be used on the simulator during this experiment.

7.2

7.2 Raman Spectroscopy

Now a days, rapid development of surface-enhanced raman scattering (SERS)-based biosensors leads to the SERS realm of applications from chemical analysis to nanostructure characterization and biomedical applications [40].

The optical method of raman spectroscopy provides information relying on the change of bond polarizability of a molecule through inelastic probing of its vibrations. Although the cross-section of raman scattering is low, it is extremely sensitive to intramolecular conditions. In addition, although water is always present as one of the elements of the biological materials, the raman spectroscopic fingerprint of biomolecules is not affected by water too much [8].

Fig. 29 Renishaw Raman Spectroscopic Machine

Therefore using RENISHAW in Via Raman spectrometer, spectra would be obtained for different synovial contents before and after tribological experiments in the simulator. Also, the surface of the balls will be observed if the chemical properties are changing with the tribological process.

To obtained the Raman data, the green laser would be used. On the surfaces of CoCrMo and ceramic ball, 1mw laser power would be used with the exposure time of 100s. The fingerprints of the lubricants before and after tribological tests would be achieved with 100mw laser power and 20s exposing time.

7.3 Interpretation of obtained results

The spectra obtained by Raman spectroscopy is a fingerprint for each compound that describes a specific chemical structure. The spectroscopic difference provided for the fluids before use and after experiment within the simulator of ball-on- cup set up can explain the result if chemical reactions are occurring in artificial joint replacement. Also, by observing the changing peaks of Raman Spectra on the ball of lubricant film formed exhibit chemical structural change taking place due to bond breaking or formation within the component of SF.

For each contact couple with SF liquids, the frictional coefficient will also be calculated within the hip joint simulator. Therefore, discussing the significant differences within the spectroscopic values along with the frictional coefficient of each experimental set could be the understanding of the lubrication mechanism of synovial liquid contents on the hip prosthesis heads.

8 CURRENT STATE OF THESIS

8.1 Raman Spectroscopic analysis

Using Renishaw inVia Raman spectrometer, the below spectra have been obtained for model synovial fluids on different implant material surfaces after tribological experiments. Besides, optical images of the film formed on CoCrMo metal ball, BIOLOX®forte and BIOLOX®delta ceramic balls were taken.

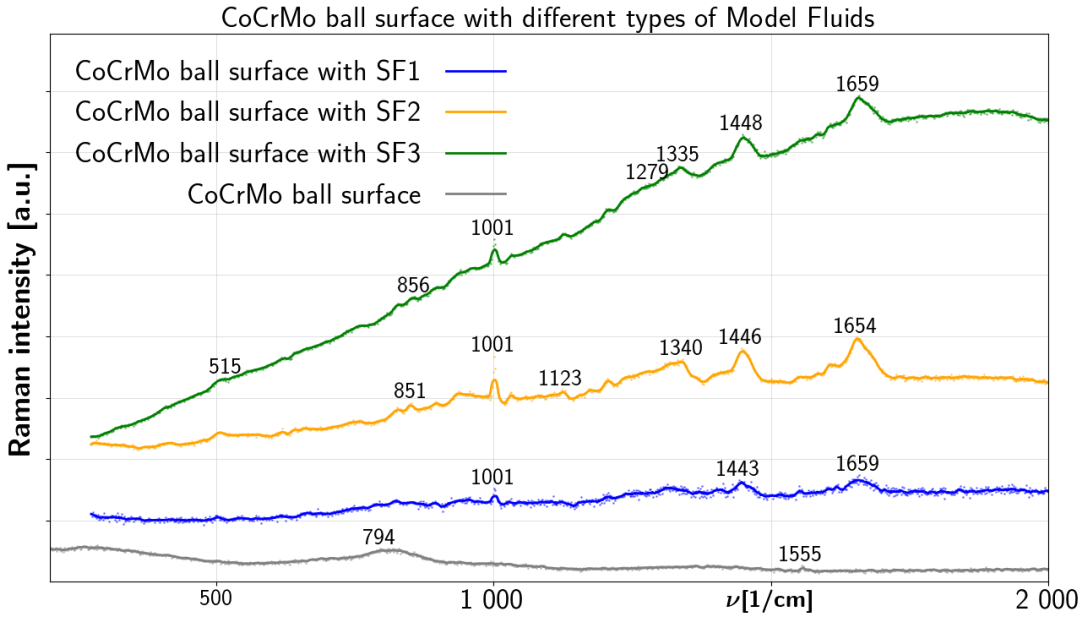

Fig. 30 Raman Spectroscopic data for SF1, SF2 and SF3 model SFs on CoCrMo ball surface

In Raman spectrum, there are several qualitative and quantitative indicators of a peptide conformation. The Amide I band describes the C=O stretching coordinates, contributions from C-N stretching and N-H deformation coordinates. In common secondary structural motifs of peptides such as α-helix or β-sheet structure, the hydrogen bodings of carbonyl groups have well-defined geometries. The position for the α-helical peptide is 1645-1660 cm^{-1}, while for β-sheet peptide, the band is located at 1665-1680 cm^{-1}. On the other hand, Amide III vibrations (describing the vibrational coupling between adjacent C-H and N-H deformation) are observed at 1265-1300 cm^{-1} for α-helix, while the β-sheet structure shifts the band to 1230-1240 cm^{-1}. Therefore, the changes of the relative composition of a peptide conformation through chemical reactions are easily monitored using Raman spectroscopy [41].

CoCrMo Surface with different model Fluid obtained Raman data, as shown in figure 30. Here for model fluid, SF1 and SF3 are showing peaks on 1659$cm^{-1,}$ while for SF2, it shifted to 1654 cm^{-1}. This range is basically the α helix Amide I range, which precisely explains the Amide I bonding for albumin [41]. Another peak range is showing 1443 cm^{-1}, 1446 cm^{-1} and 1448 cm^{-1}, respectively for SF1, SF2 and SF3. while this range may occur due to CH_2/CH_3 deformation [13, 42].

Here SF2 and SF3 is showing a peak in 1340 cm^{-1} and 1335 $cm^{-1,}$ respectively, while SF1 is not showing any peak in this range, this range provides information regarding CH_2-CH_3 wagging [13, 42]. Only SF3 is showing a peak in 1279 cm^{-1} that is within the range of Amide III α helix [41]. Only SF2 is showing spectra 1123 cm^{-1}, basically gives information about the protein backbone. Thus, this peak is due to C-C, C-OH, C-N stretch, C-O-C, glycosidic linkage [13].

1001 cm^{-1} is the peak found in SF1, SF2 and SF3, due to ring breathing [13, 42]. SF2 and SF3 is providing the peak of 851 cm^{-1} and 856 $cm^{-1,}$ which due to C-C Skeletal stretch [42]. 515 cm^{-1} peak showing in SF3 probably due to the tertiary and quaternary branched carbon atom next to the tertiary carbon atom [42].

While these above-described peaks do not match with any peaks that occur within the CoCrMo surface, such as 1555 cm^{-1} and 794 cm^{-1}. For all three model fluids α helix Amide I and for SF3 α-helix Amide III are attached to the surface. Thus, albumin is attached here on the CoCrMo surface, probably.

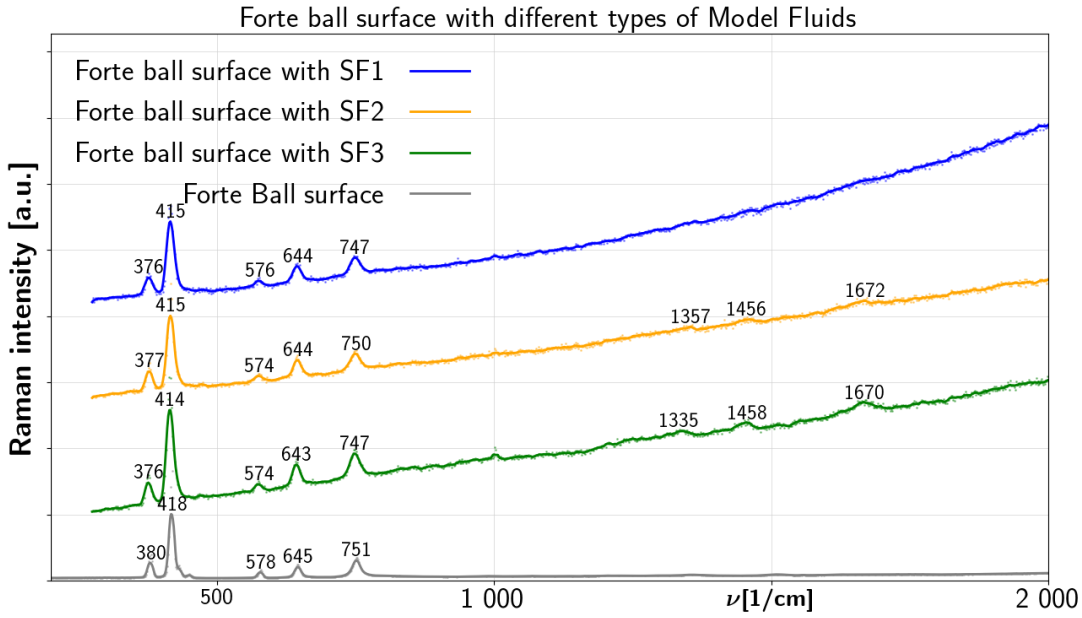

Fig. 31 Raman Spectroscopic data for SF1, SF2 and SF3 model SFs on BIOLOX®forte ball surface

BIOLOX®forte ball surface with all three model fluid data is shown in figure 31. For Synovial model fluid SF1 and SF3 on the ball surface, 751 $cm^{-1,}$ the peak of the clean BIOLOX®forte ball is shifting 747 cm^{-1} and for SF2 shifting in 750 cm^{-1}. The spectra were found in 645 cm^{-1} for without test ball surface after testing with fluid SF1, SF2 and SF3 found in 644 cm^{-1}, 644 cm^{-1} and 643 cm^{-1}, respectively. As present in the clear BIOLOX®forte surface, a peak around 578 cm^{-1} is visible also within BIOLOX®forte surface after test with all three fluids for SF1, SF2 and SF3 in the order 576 cm^{-1}, 574 cm^{-1} and 574 cm^{-1}. The peak 418 cm^{-1} of the clear surface peak is shifting in 415 cm^{-1} for SF1 and SF2 and in 414 cm^{-1} for SF3, respectively. All three fluids on the BIOLOX®forte surface are also showing peak near 380 cm^{-1} of

the clear ball, 376 cm^{-1} for SF1 and SF3, 377 cm^{-1} for SF2. But the notable peaks are observable here on the BIOLOX®forte ball surface is 1335 cm^{-1}, 1458 cm^{-1} and 1670 cm^{-1} peaks found for after testing with SF3 and after testing with SF2 is showing differences in 1357 cm^{-1}, 1456 cm^{-1} and 1672 cm^{-1}.

The BIOLOX®forte ball surface remains unchanged mostly while testing with the SF of a healthy joint. However, the BIOLOX®forte ball surface shows three remarkable peaks while testing with SF2 and SF3 that is the SF of total joint replacement and osteoarthritic joint, respectively. 1456 cm^{-1} and 1458 cm^{-1} give information about CH_2/CH_3 deformation [13, 42]. The peak 1357 cm^{-1} and 1335 cm^{-1} are due to CH_2-CH_3 wagging, showing by SF2 and SF3 model fluid data [13, 42]. Furthermore, 1672 cm^{-1} and 1670 cm^{-1} peak observed on the BIOLOX®forte surface are providing information about Amide I of the β sheet structure. The above discussion proves that BIOLOX®forte is chemically attached or adsorbing γ-globulin from osteoarthritic joint and SF from total joint replacement.

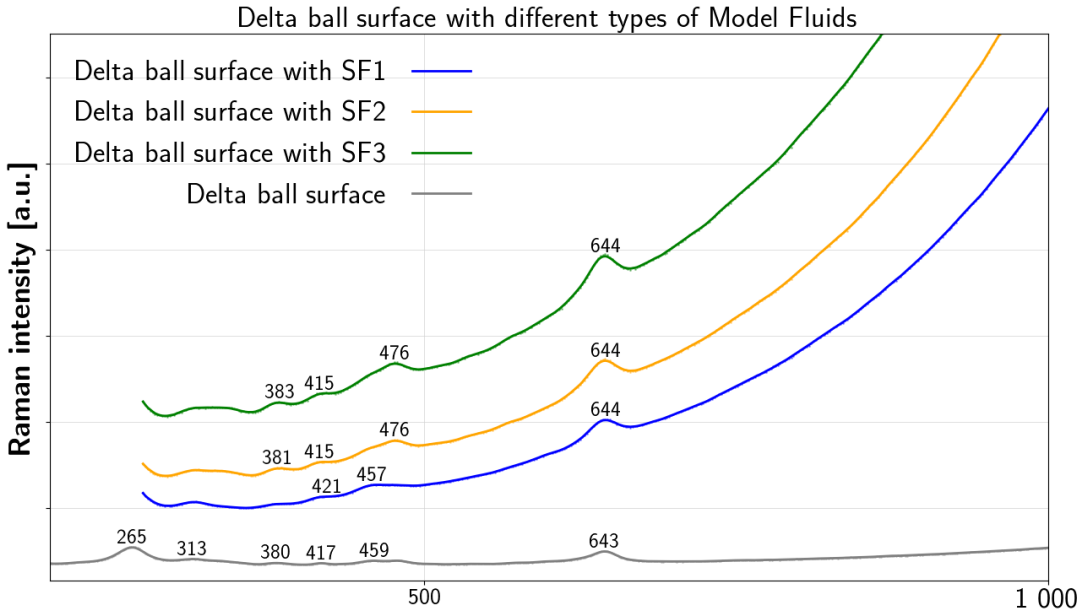

Fig. 32 Raman Spectroscopic data for SF1, SF2 and SF3 model SFs on BIOLOX®delta ball surface

Figure 32 is showing the BIOLOX®delta surface with all three model fluids SF1, SF2 and SF3. The clean BIOLOX®delta surface contents are proving the peaks 265 cm^{-1}, 313 cm^{-1}, 380 cm^{-1}, 417 cm^{-1}, 459 cm^{-1} and 643 cm^{-1}. The peak in 644 cm^{-1} is showing for all three model fluids on the BIOLOX®delta ball surface are shifted from peak 643 cm^{-1} of the clean ball. 457 cm^{-1} for SF1 on the ball surface and 476 cm^{-1} for both SF2 and SF3 on the ball surface are comparable with the clear ball surface peak 459 cm^{-1}. The peaks 421 cm^{-1}, 415 cm^{-1} and 415 cm^{-1} respectively for SF1, SF2 and SF3 fluids on the BIOLOX®delta surface are shifted from 417 cm^{-1} of the clean ball. Moreover, the peak found in 380 cm^{-1} is observed after testing with SF2 in 381 cm^{-1} and after testing with SF3 in 383 cm^{-1}. All three types of model

fluids did not exhibit any perceptible change of their chemical structures after the test with this ceramic ball. The BIOLOX®delta ball surface remains more or less the same after-test with all these types of fluids. Thus, for the tribological test of model SFs with BIOLOX®delta ball, it can be assumed that there is no reaction between model SF and the BIOLOX®delta ball surface within simulator.

Therefore, surface-enhanced Raman scattering (SERS)-based biosensors are developing rapidly for the applications of chemical analysis, nanostructure characterization, as well as for biomedical sectors [40]. Making use of a high increase of Raman signal after protein binding to the metallic nanoparticle(s), SERS is an effective technique, especially for the molecules on a metal surface [42, 43, 44]. In another SERS study of protein–nanoparticle interaction, bio-conjugated silver nanoparticles were used by Laruinaz et al. [45]. In summary, SERS has been recognized a very successful operative analytical tool due to its high sensitivity, high selectivity, and fluorescence-quenching properties [40, 45].

8.2 Coefficient of friction analysis

8.2

The coefficient of friction measurement took place for all the model SFs with CoCrMo and polyethylene contact pair and BIOLOX®delta and BIOLOX®forte ceramic contact pairs. It is observed that for SF1, BIOLOX®forte exhibits the highest frictional coefficient and BIOLOX®delta showed the lowest. While for SF3, BIOLOX®forte shows the lowest frictional coefficient value and CoCrMo shows the highest.

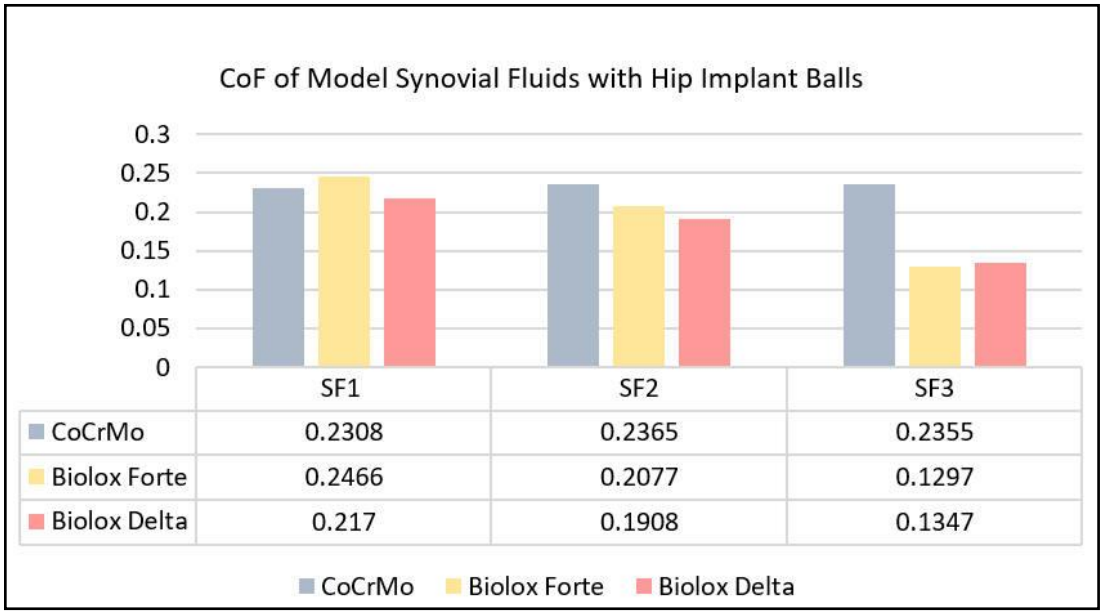

Fig. 33 Coefficient of friction for CoCrMo and Polyethylene, BIOLOX®forte and BIOLOX®delta contact pairs respectively for SF1, SF2 and SF3 model synovial fluids.

Both ceramic contact pairs show a higher value for SF1 and lower value for SF3, while SF2 ranges for ceramics are somewhere in the middle. But for CoCrMo, all the Coefficient of frictions values are very close and all are above 0.23. However, The

coefficient of friction for model fluids with different hip implants could not be correlated with chemical changes significantly.

8.3

8.3 Formed Film structure

Formed film structures on CoCrMo and ceramic ball surfaces by all three model SF were observed by microscope of the Raman spectroscopic machine to investigate the influence of the film structures due to chemical reaction.

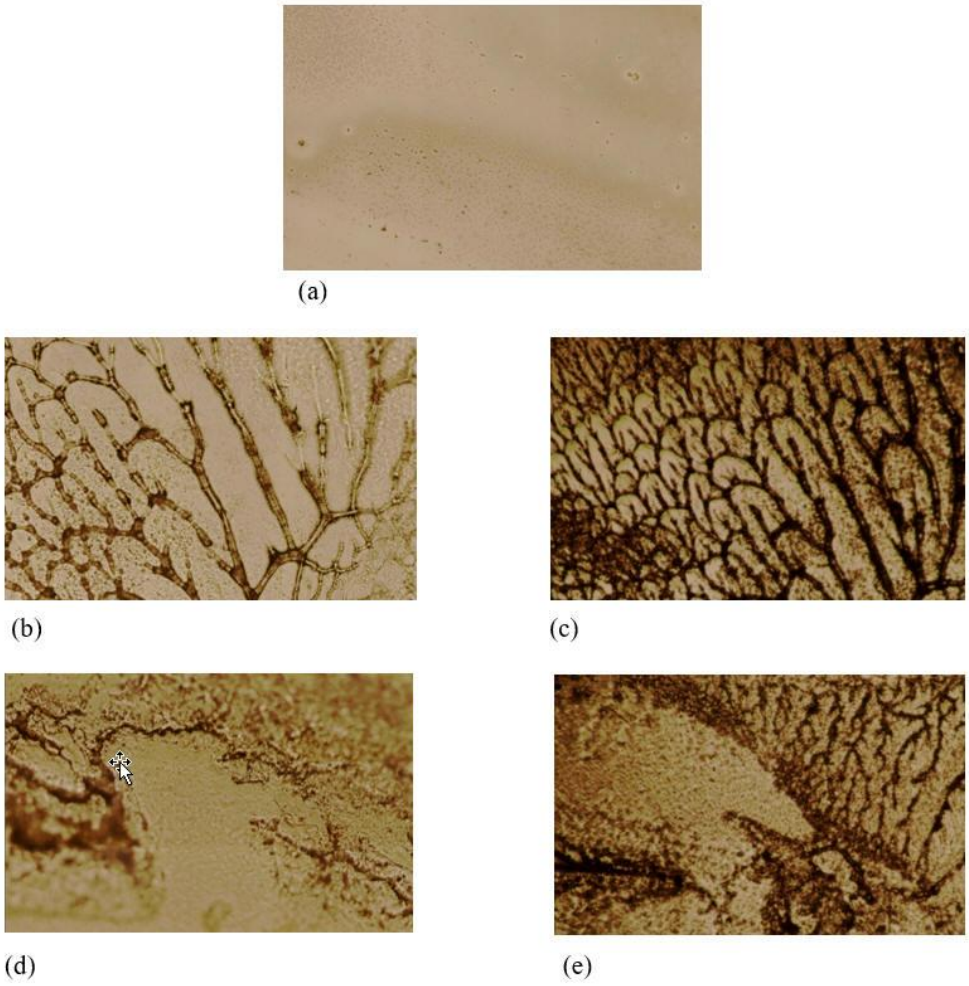

Fig. 34 CoCrMo ball viewed by Raman Microscope, respectively (a) SF1 on the surface, (b) and (c) SF2 on the surface, (d) and (e) SF3 on the surface. The horizontal sizes of panels are 20µm for (a), (b) and (d). The horizontal sizes of panels are 5µm for (c) and (e).

The different structures of the formed film produced by different model SFs are clearly visible from the above pictures. Thus, these observations can also play an essential role in the biochemical explanation of adsorption taking place on the metal surface by SF molecules during film formation.

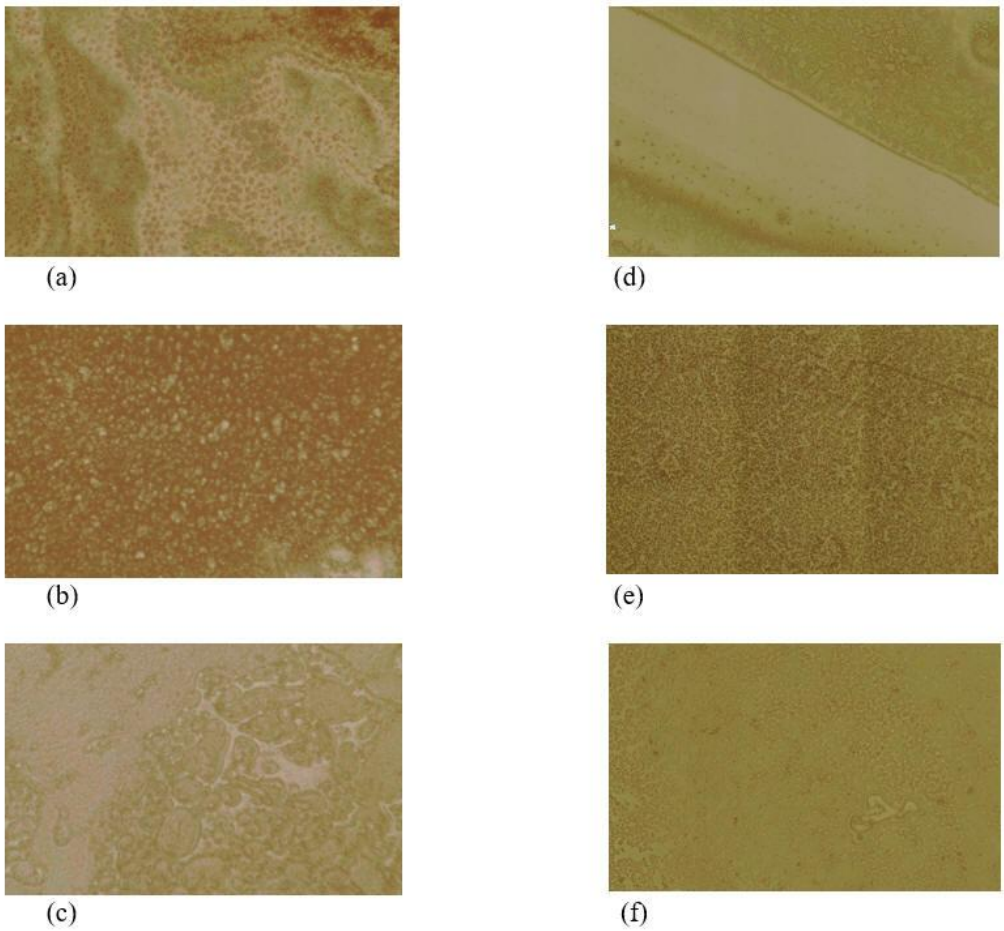

Fig. 35 Ceramic ball viewed by Raman Microscope respectively (a) SF1 on BIOLOX®delta (b) SF2 on BIOLOX®delta (c) SF3 on BIOLOX®delta (d) SF1 on BIOLOX®forte (e) SF2 on BIOLOX®forte (f) SF3 on BIOLOX®forte.). The horizontal size of panels are 5µm for (a), (b) and (c) and 20 µm for (d), (e)and (f).

During observation of the surface of ceramic balls by microscope after tribological tests by simulator above views were found. There was not much crystallization observed as viewed in the case of metal balls. Finally, it could be observed as each type of model fluids changes the characteristics of the film on the implant surfaces. When the concentration of the elements of SF is changing, the pattern of developed film is also changing.

9 CONCLUSIONS

Therefore, to describe the condition of joint replacement and to increase the longevity of the replaced area, the chemical changes taking place in the synovial fluid need to be observed to explain the biochemical behavior of the materials using in joint replacement. Raman spectroscopy is an excellent technique to understand clearly the changes of the chemical structure, as Raman spectra contain the fingerprint of each compound that describes a specific chemical structure within the formed film. By observing the Raman spectra of lubricant film formed on the ball, it is possible to address the chemical structural changes that are taking place within the synovial fluid.

Hence, tribological experiments were carried out for metal and ceramic implants with three types of model SFs. These are SF of a healthy joint, SF after total joint replacement and SF of the osteoarthritic joint. It was revealed that on the CoCrMo surface, albumin is chemically adsorbed from all three types of model fluids. However, the BIOLOX®forte ball surface shows chemisorption of γ-globulin in case of testing with SF2 and SF3 that is the SF of total joint replacement and osteoarthritic joint, respectively. While BIOLOX®delta remains unchanged after test with all three types of model SFs. In the microscopic view of the implant surface showed in case of the concentration of the components of SF are changing, the developed film patterns are also changing. Nevertheless, the coefficient of friction with all these lubricants could not be correlated with chemisorption occur within the contact pairs.

Furthermore, Raman analysis of all three model SF liquid and separately all the components of SF, before and after tribological test with different implants, may show significant spectroscopic differences. Consequently, it would be possible to understand the lubrication chemistry and mechanism of synovial liquid within prosthesis more explicitly.

10

10 COOPERATION WITH OTHER INSTITUTIONS

In order to conduct the research as mentioned above, it is planned to collaborate with the institution below.

- Mgr. Dusan Hemzal, Ph.D.

Ustav Fyziky Kondenzovanych Latek
Masarykova Univerzita
Kotlarska 2, 611 37 Brno, Czech Republic.

- Renishaw Invia setup
- Raman Spectroscopic Measurement
- Preparation of Protein Capillaries

- Ing. Dipankar Choudhury, Ph.D.

Nano Mechanics and Tribology Laboratory
Department of Mechanical Engineering
University of Arkansas, Fayetteville, AR, USA.

- Observation of Analysis
- Expert Consultancy

11 REFERENCES

[1] Bennike, Tue, Ugur Ayturk, Carla M. Haslauer. et al. A normative study of the synovial fluid proteome from healthy porcine knee joints. *Journal of proteome research*, 2014, 13.10: 4377-4387.

[2] Greene, G. W., X. Banquy, D. W. Lee, D. D. Lowrey, J. Yu & J. N.Israelachvili. Adaptive mechanically controlled lubrication mechanism found in articular joints. *Proceedings of the National Academy of Sciences*, 2011, 108.13: 5255-5259.

[3] Zhang, Z., S. Barman & G. F. Christopher. The role of protein content on the steady and oscillatory shear rheology of model synovial fluids. *Soft matter*, 2014, 10.32: 5965-5973.

[4] Fan Jingyun, Connor Myant, Richard Underwood & Philippa Cann. Synovial fluid lubrication of artificial joints: protein film formation and composition. *Faraday discussions*, 2012, 156.1: 69-85.

[5] Kitano Toshio, Gerard A Ateshian, Van C Mow, Yoshinori Kadoya & Yoshiki Yamano. Constituents and pH changes in protein rich hyaluronan solution affect the biotribological properties of artificial articular joints. *Journal of biomechanics*, 2001, 34.8: 1031-1037.

[6] Walker P.S , Sikorski J, Dowson D, Longfield M D, Wright V & Buckley T. Behaviour of synovial fluid on surfaces of articular cartilage. A scanning electron microscope study. *Annals of the rheumatic diseases*, 1969, 28.1: 1.

[7] Blewis ME, GE Nugent-Derfus, TA Schmidt, BL Schumacher and RL Sah. A model of synovial fluid lubricant composition in normal and injured joints. *European cells and Materials*, 2007, 13.1: 26-39.

[8] Depciuch Joanna, Magdalena Sowa-Kućma, Gabriel Nowak, Dominika Dudek, Marcin Siwek, Krzysztof Styczeń & Magdalena Parlińska-Wojtan. Phospholipid-protein balance in affective disorders: Analysis of human blood serum using Raman and FTIR spectroscopy. A pilot study. *Journal of Pharmaceutical and Biomedical Analysis.* 2016, 131, 287-296.

[9] Hills B. A. & R.W. Crawford. Normal and prosthetic synovial joints are lubricated by surface-active phospholipid. *The Journal of arthroplasty*, 2003, 18.4: 499-505.

[10] Ghosh, Subir, Dipankar Choudhury, Nabangshu Shekhar Das & Belinda Pingguan Murphy. Tribological role of synovial fluid compositions on artificial joints - a systematic review of the last 10 years. *Lubrication Science*, 2014, 26.6: 387-410.

[11] Galandáková Adéla, Jitka Ulrichová, Kateřina Langová, Adéla Hanáková, Martin Vrbka, Martin Hartl & Jiri Gallo. Characteristics of synovial fluid required

for optimization of lubrication fluid for biotribological experiments. *Journal of Biomedical Materials Research Part B: Applied Biomaterials*, 2017, 105.6: 1422-1431.

[12] Park Jong-Bong, Cong-Truyen Duong, Ho-Geun Chang, et al. Role of hyaluronic acid and phospholipid in the lubrication of a cobalt–chromium head for total hip arthroplasty. *Biointerphases*, 2014, 9.3: 031007.

[13] Esmonde-White, Karen A., Gurjit S. Mandair, Farhang Raaii, Jon A. Jacobson, Bruce S. Miller, Andrew G. Urquhart, Blake J. Roessler A Michael D. Morris. Raman spectroscopy of synovial fluid as a tool for diagnosing osteoarthritis. *Journal of biomedical optics*, 2009, 14.3: 034013.

[14] Mazzucco Dan, Richard Scott & Myron Spector. Composition of joint fluid in patients undergoing total knee replacement and revision arthroplasty: correlation with flow properties. *Biomaterials*, 2004, 25.18: 4433-4445.

[15] Nečas David, Martin Vrbka, Filip Urban, Ivan Křupka & Martin Hartl. The effect of lubricant constituents on lubrication mechanisms in hip joint replacements. *Journal of the mechanical behavior of biomedical materials*, 2016, 55: 295-307.

[16] Duong Cong-Truyen, Jae-Hoon Lee, Younho Cho, Ju-Suk Nam, Hyong-Nyun Kim, Sang-Soo Lee & Seonghun Park. Effect of protein concentrations of bovine serum albumin and γ-globulin on the frictional response of a cobalt-chromium femoral head. *Journal of Materials Science: Materials in Medicine*, 2012, 23.5: 1323-1330.

[17] Cawley, J., J.E.P. Metcalf, A.H. Jones, T.J. Band & D.S. Skupien. A tribological study of cobalt chromium molybdenum alloys used in metal-on-metal resurfacing hip arthroplasty: note ii. *Wear*, 2003, 255.7-12: 999-1006.

[18] Nečas, D., Vrbka, M., Křupka, I., & Hartl, M. The Effect of Kinematic Conditions and Synovial Fluid Composition on the Frictional Behaviour of Materials for Artificial Joints. *Materials*, 2018, 11.5: 767.

[19] Nečas David, M. Vrbka, D. Rebenda, J. Gallo, A. Galandáková, L. Wolfová, I. Křupka & M. Hartl. In situ observation of lubricant film formation in THR considering real conformity: The effect of model synovial fluid composition. *Tribology International*, 2018, 117: 206-216

[20] Jemma G. Kerns, Panagiotis D. Gikas, Kevin Buckley, Adam Shepperd, Helen L. Birch, Ian McCarthy, Jonathan Miles, Timothy W. R. Briggs, Richard Keen, Anthony W. Parker, Pavel Matousek, and Allen E. Goodship. Evidence from raman spectroscopy of a putative link between inherent bone matrix chemistry and degenerative joint disease. *Arthritis & Rheumatology*, 2014, 66.5: 1237-1246.

[21] Taddei Paola, Modena Enrico, Traina Francesco & Saverio Affatato. Raman and fluorescence investigations on retrieved Biolox® delta femoral heads. *Journal of Raman Spectroscopy*, 2012, 43.12: 1868-1876.

[22] Parkes Maria, Connor Myant, Philippa M. Cann & Janet S.S. Wong. Synovial Fluid Lubrication: The Effect of Protein Interactions on Adsorbed and Lubricating Films. *Biotribology*, 2015, 1: 51-60.

[23] Vrbka Martin, Ivan Křupka, Martin Hartl, Tomáš Návrat, Jiří Gallo & Adéla Galandáková. In situ measurements of thin films in bovine serum lubricated contacts using optical interferometry. *Proceedings of the Institution of Mechanical Engineers, Part H: Journal of Engineering in Medicine*, 2014, 228.2: 149-158.

[24] Parkes Maria, Connor Myant, Philippa M. Cann & Janet S.S. Wong. The effect of buffer solution choice on protein adsorption and lubrication. *Tribology International*, 2014, 72: 108-117.

[25] Schmidt, Tannin A., Nicholas S. Gastelum, Quynhhoa T. Nguyen, Barbara L. Schumacher & Robert L. Sah. Boundary Lubrication of Articular Cartilage: Role of Synovial Fluid Constituents. *Arthritis & Rheumatism*, 2007, 56.3: 882-891.

[26] Nakashima Kazuhiro, Yoshinori Sawae, Teruo Murakami & Stefano Mischler. Behavior of Adsorbed Albumin Film on CoCrMo Alloy under In-situ Observation. *Tribology Online*, 2015, 10.2: 183-189

[27] Zhu Wenliang, Elia Marin, Nobuhiko Sugano, & Guiseppe Pezzotti. Tensor-resolved Raman spectroscopic analysis of wear-induced residual stress fields in long-term alumina hip-joint retrievals. *Journal of the mechanical behavior of biomedical materials*, 2017, 66: 201-210.

[28] Choudhury Dipankar, Matus Ranuša, Robert A. Fleming, Martin Vrbka, Ivan Křupka, Matthew G. Teeter, Josh Goss & Min Zou. Mechanical Wear and Oxidative Degradation Analysis of Retrieved Ultra High Molecular Weight Polyethylene Acetabular Cups. *Journal of the mechanical behavior of biomedical materials*, 2018, 79: 314-323.

[29] Navarro M, A. Michiardi, O. Castano & J.A. Planell. Biomaterials in orthopaedics. *Journal of the Royal Society Interface*, 2008, 5.27: 1137-1158.

[30] Buckwalter JA, Mankin HJ. Articular cartilage. Part II: degeneration and osteoarthrosis, repair, regeneration, and transplantation. *J Bone Joint Surg Am*, 1997, 79.4: 612-632

[31] Sun D., J.A. Wharton, R.J.K. Wood, L. Ma & W.M. Rainforth. Microabrasion–corrosion of cast CoCrMo alloy in simulated body fluids. *Tribology International*, 2009, 42.1: 99-110.

[32] Contu F., B. Elsener A H. Böhni. Characterization of implant materials in fetal bovine serum and sodium sulfate by electrochemical impedance spectroscopy. II. Coarsely sandblasted samples. *Journal of Biomedical Materials Research Part A: An Official Journal of The Society for Biomaterials, The Japanese Society for Biomaterials, and The Australian Society for Biomaterials and the Korean Society for Biomaterials*, 2003, 67.1: 246-254.

[33] Valero Vidal C. & A. Igual Muñoz. Study of the adsorption process of bovine serum albumin on passivated surfaces of CoCrMo biomedical alloy. *Electrochimica Acta*, 2010, 55.28: 8445-8452.

[34] Yan Yu, Anne Neville & Duncan Dowson. Biotribocorrosion of CoCrMo orthopaedic implant materials—Assessing the formation and effect of the biofilm. *Tribology international*, 2007, 40.10-12: 1492-1499.

[35] Vrbka, M., D. Nečas, M. Hartl, I. Křupka, F. Urban & J. Gallo. Visualization of lubricating films between artificial head and cup with respect to real geometry. *Biotribology*, 2015, 1: 61-65.

[36] Choudhury Dipankar, Filip Urban, Martin Vrbka, Martin Hartl & Ivan Krupka. A novel tribological study on DLC-coated micro-dimpled orthopedics implant interface. *Journal of the mechanical behavior of biomedical materials*, 2015, 45: 121-131.

[37] Nečas, D., Vrbka, M., Urban, F., Gallo, J., Křupka, I., & Hartl, M. In situ observation of lubricant film formation in THR considering real conformity: The effect of diameter, clearance and material. *Journal of the mechanical behavior of biomedical materials*, 2017, 69: 66-74.

[38] Nečas, D., Usami, H., Niimi, T., Sawae, Y., Křupka, I., & Hartl, M. Running-in friction of hip joint replacements can be significantly reduced: The effect of surface-textured acetabular cup. *Friction*, 2020, 22: 1-6.

[39] Furmann, D., Nečas, D., Rebenda, D., Čípek, P., Vrbka, M., Křupka I & Hartl, M. The Effect of Synovial Fluid Composition, Speed and Load on Frictional Behaviour of Articular Cartilage. *Materials*, 2020, 13.6: 1334.

[40] Han Xiao X., Bing Zhao & Yukihiro Ozaki. Surface-enhanced Raman scattering for protein detection. *Analytical and bioanalytical chemistry*, 2009, 394.7: 1719-1727.

[41] Diem Max. Modern vibrational spectroscopy and micro-spectroscopy: Theory, instrumentation and biomedical applications. John Wiley & Sons, 2015.

[42] Lin-Vien D, Colthup NB, Fateley WG, Grasselli JG. The handbook of infrared and Raman characteristic frequencies of organic molecules. Elsevier, 1991.

[43] Zou Shouzhong & Michael J. Weaver. Surface-Enhanced Raman Scattering on Uniform Transition-Metal Films: Toward a Versatile Adsorbate Vibrational Strategy for Solid-Nonvacuum Interfaces? *Analytical chemistry*, 1998, 70.11: 2387-2395.

[44] Shanmukh Saratchandra, Les Jones, Jeremy Driskell, Yiping Zhao, Richard Dluhy & Ralph A. Tripp. Rapid and Sensitive Detection of Respiratory Virus Molecular Signatures Using a Silver Nanorod Array SERS Substrate. *Nano letters*, 2006, 6.11: 2630-2636.

[45] Reymond-Laruinaz Sébastien, Lucien Saviot, Valérie Potin & María Del Carmen Marco De Lucas. Protein–nanoparticle interaction in bioconjugated silver nanoparticles: A transmission electron microscopy and surface enhanced Raman spectroscopy study. *Applied Surface Science*, 2016, 389: 17-24.

12

12 LIST OF FIGURES AND TABLES

13 LIST OF USED ABBREVIATIONS

SF	Synovial fluid
PLs	Phospholipids
HA	Hyaluronic acid
PRG4	Proteoglycan 4
SAPL	Surface active phospholipids
OA	Osteoarthritis
PBS	Phosphate- buffered saline
BSA	Bovine serum albumin
BGG	Bovine gamma globulin
NaOH	Sodium hydroxide
HCl	Hydrogen chloride
CoCrMo	Cobalt chromium molybdenum
BS	Bovine serum
TJR	Total joint replacements
AFM	Atomic force microscopy
DPPC	Dipalmitoylphosphatidylcholine
LUB	Glycoprotein lubricin
UHMWPE	Ultra-high molecular weight polyethylene
(K/L) Scores	Kellgren/Lawrence Scores
DPRS	Drop deposition/Raman Spectroscopy protocol
PE	Polyethylene
Vm	Monoclinic volume fraction
TKA	Total knee arthroplasty
SERS	Surface-enhanced raman scattering